shown) and was inhibited by the addition of a 10-fold excess of unlabeled NMU-25 as a competitor (Fig. 4*C*, *top* and *bottom*), suggesting the specific interaction of NMU-25 to these cells.

Biologically active ligands for GPCRs have been reported to bind specifically to their cognate receptors and cause an increase in second messengers such as intracellular-Ca^{2+} and/or cAMP levels. We therefore determined the ability of NMU for the induction of these second messengers in LC319 cells through its interaction with GHSR1b/NTSR1. Enhancement of cAMP production (Fig. 4*D*), but not of Ca^{2+} flux, was detected by NMU-25 in a dose-dependent manner in LC319 cells that expressed both GHSR1b and NTSR1, when the cells were cultured in the presence of NMU-25 in final concentrations of 3 to 100 μmol/L in the culture media (data not shown). The results showed that NMU-25 activated the NMU-25-related signaling pathway possibly through functional GHSR1b/NTSR1 in NSCLC cells. This effect was likely to be NMU-25-specific, because the addition of the same amount of GHRL and NTS, known ligands for GHSR/NTSR1, did not enhance cAMP production (Fig. 4*D*). On the other hand, treatment with NTS, but not that with GHRL, caused the mobilization response of intracellular Ca^{2+} in LC319 cells (data not shown), similar to previous reports (23, 24), suggesting the ligand-dependent and diverse physiologic function of GHSR1b and/or NTSR1 in mammalian cells.

We then examined the biological significance of the NMU-receptor interaction in pulmonary carcinogenesis using plasmids designed to express siRNA against *GHSR* or *NTSR1* (si-*GHSR-1*, si-*NTSR1-1*, and si-*NTSR1-2*). Transfection of either of these plasmids into LC319 or A549 cells suppressed the expression of the endogenous receptor in comparison with cells containing any of the three control siRNAs (Supplementary Fig. S4, *top*). In accordance with the reduced expression of the receptors, LC319 and A549 cells showed significant decreases in cell viability and number of colonies (Supplementary Fig. S4, *middle* and *bottom*). These results strongly support the possibility that NMU, by interaction with GHSR1b and NTSR1, might play a very significant role in the development/progression of lung cancer.

Internalization of GHSR1b/NTSR1 receptors after binding with NMU. To determine the mechanism involved in the regulation

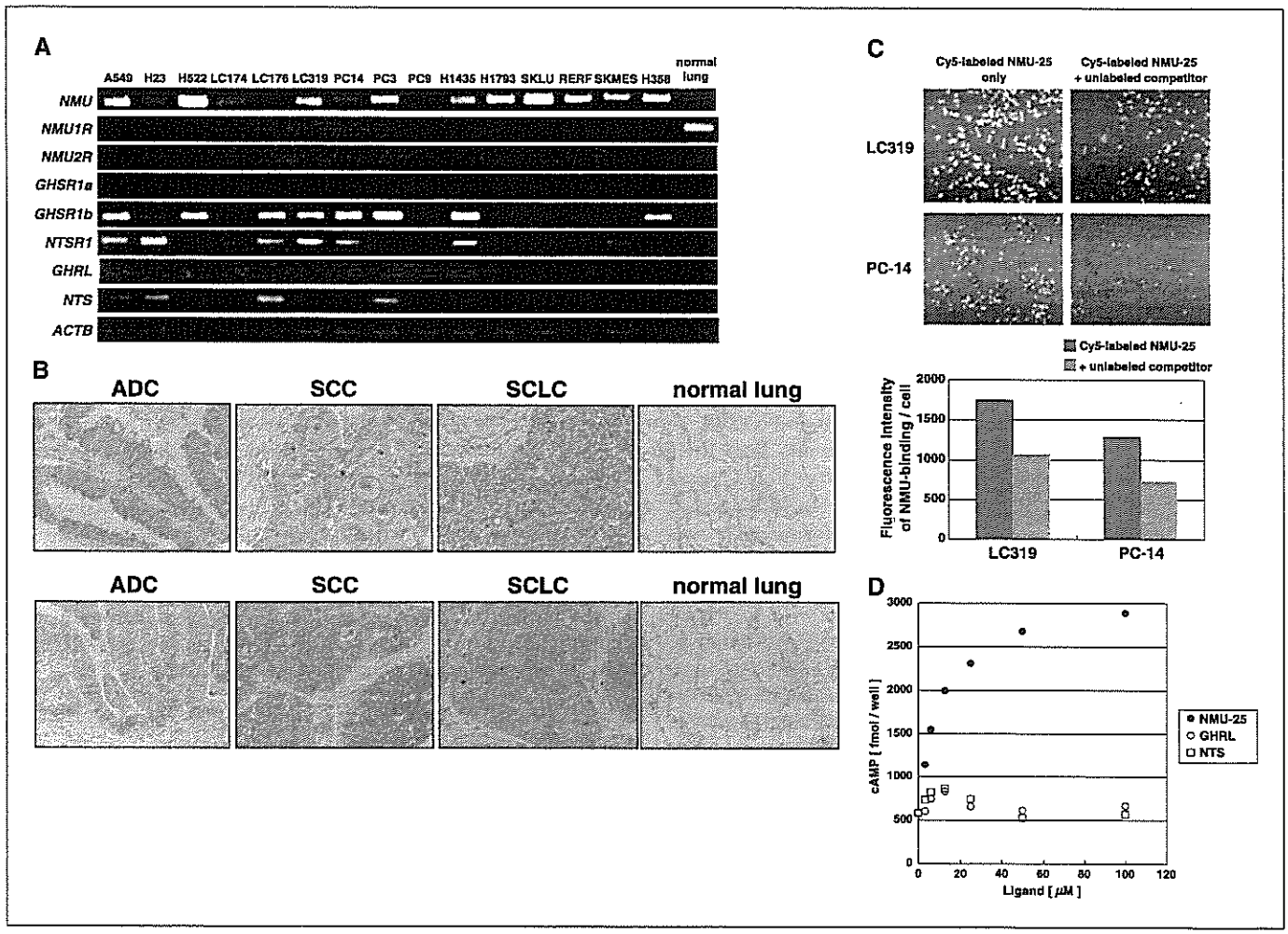

Figure 4. Functional association of NMU with endogenous GHSR1b/NTSR1 on the NSCLC cells. *A*, expression of *NMU*, candidate receptors, and their known ligands as detected by semiquantitative RT-PCR analysis in NSCLC cell lines. *B*, immunohistochemical staining of representative surgically resected and autopsy samples including NSCLC [lung adenocarcinoma (ADC) and squamous cell carcinoma (SCC)] and SCLC as well as normal lung, using anti-NTSR1 (*top*) or anti-GHSR1b (*bottom*) antibody (original magnification, ×200). *C*, binding of Cy5-labeled NMU-25 to the cell surface of NSCLC cells analyzed by laser scanning imaging. Digital fluorescence images of Cy5-labeled NMU-25 (1 μmol/L) bound to LC319 and PC14 cells with/without 10 μmol/L of nonlabeled NMU-25 peptides as a competitor was detected by the 8200 Cellular Detection System (*top*). *Columns*, the average fluorescence values of Cy5-labeled NMU-25 bound to each cell in duplicate assays (*bottom*). *D*, specific signal transduction by NMU as represented by cAMP release in LC319 cells. Dose-response curves of intracellular cAMP production by NMU-25 (●), GHRL (○), or NTS (□) treatment (3-100 μmol/L) in LC319 cells were shown.

of NMU-GHSR1b/NTSR1 signaling, we examined whether GHSR1b/NTSR1 is internalized when they are exposed to NMU, through confocal microscopy observation of the subcellular distribution of the two receptors after NMU-25 stimulation. After they were introduced in COS-7 cells, the GHSR1b and NTSR1 receptors were mainly colocated at the plasma membrane in the condition without the exposure to NMU-25. However, once NMU-25 was added to the cell culture, both of the receptors were cointernalized and predominantly formed the vesicle-like structures in a time-dependent manner (Fig. 5*A*). Similarly, in LC319 cells, in which GHSR1b and NTSR1 were endogenously overexpressed, NMU stimulation induced the cointernalization of the two receptors (Supplementary Fig. S5). The results suggest the possible physical interaction between GHSR1b and NTSR1, as well as NMU-induced cointernalization.

To further confirm whether NMU is internalized after binding to its receptors, internalization of NMU was investigated using Alexa Fluor 594–labeled NMU-25 (NMU-25-Alexa 594) and a confocal microscopy. The binding of agonists to GPCRs on the cell surface is generally known to initiate receptor-mediated endocytosis. In the course of this process, receptors are passed through multiple intracellular pathways that lead to lysosomal degradation or recycling them to the cell surface (25, 26). On the other hand, far less is known about whether all GPCR ligands are internalized together with their receptor. In the case of neuropeptides, the ligand is usually internalized with its receptor (27, 28). As shown in Fig. 5*B*, the *xz*- and *yz*-projections indicated that NMU-25-Alexa 594 was incorporated within the cells. After 15 minutes of incubation, the internalized ligand was concentrated in dots or irregular clusters at more peripheral parts of the cytoplasm in cells (Fig. 5*B*, *left*). In contrast, after 45 minutes of incubation, fluorescence was concentrated within small spots clustered in the center of the cells, close to the nucleus (Fig. 5*B*, *right*). These results are similar to the previous reports demonstrating that internalization of NTS proceeded through small endosome-like organelles and the internalized ligand to accumulate at the core of the cell surrounding the nucleus (29).

Functional receptor dimerization of GHSR1b and NTSR1. To examine the direct association between GHSR1b and NTSR1, we transiently expressed either FLAG-tagged GHSR1b or FLAG-tagged NTSR1 individually, and also coexpressed both the FLAG-tagged receptors in COS-7 cells (representative data for GHSR1b was shown in Fig. 5*C*). COS-7 cells were confirmed by semiquantitative RT-PCR analysis to endogenously express both *GHSR1b* and *NTSR1*, but not NMU. Cell lysates preincubated with the cross-linking reagent were immunoprecipitated by anti-FLAG antibody, and were served for Western blot analysis using anti-FLAG, anti-NTSR1, or anti-GHSR antibody. We found coprecipitation of the following proteins: the GHSR1b monomer (~30 kDa), the NTSR1 monomer (~45 kDa), the GHSR1b/NTSR1 heterodimer (~70-75 kDa), the GHSR1b homodimer (~60-65 kDa), and the NTSR1 homodimer (~90-95 kDa; Fig. 5*C*). No such species were detected when empty vector (mock) was transfected to COS-7 cells as a negative control. In the cells expressing only FLAG-tagged NTSR1 and those coexpressing both the FLAG-tagged receptors (NTSR1 and GHSR1b), similar results were observed (data not shown). These results confirm an interaction between GHSR1b and NTSR1, implying the existence of a GHSR1b/NTSR1 heterodimer.

To further confirm the functional importance of the activation and heterodimerization of GHSR1b and NTSR1 at the signal transduction level, we examined the dose-dependent intracellular cAMP production by NMU-25 in lung cancer cell lines representing various expression patterns of the two receptors as detected by semiquantitative RT-PCR analysis (Fig. 5*D*). In LC319 cells expressing high levels of both receptors, treatment with NMU-25 resulted in a marked and reproducible cAMP accumulation (Fig. 5*D*, *top left*). RERF-LC-AI cells expressing low levels of both receptors, showed significant but low cAMP production in response to NMU-25 (Fig. 5*D*, *top right*). NCI-H358 and SK-MES-1 cells expressing either of the receptors did not show detectable cAMP production (Fig. 5*D*, *bottom*).

Identification of downstream genes of NMU. To further elucidate the NMU-signaling pathway, siRNA against *NMU* (si-*NMU*) or LUC (control siRNA) were transfected into LC319 cells overexpressing *NMU*, and genes that were down-regulated in the former cells were screened using a cDNA microarray containing 32,256 genes. By this approach, we selected 70 genes whose expression was significantly decreased in accordance with *NMU* suppression by performing the self-organizing map clustering analysis (22). Semiquantitative RT-PCR analysis confirmed the reduction of candidate transcripts in a time-dependent manner in LC319 cells transfected with si-*NMU*, but not with control siRNA for LUC (Fig. 6*A*). We also evaluated the transactivation of these genes in accordance with the introduction of *NMU* expression in lung cancer cell lines (data not shown) and finally identified six candidate NMU-target genes, *FOXM1, GCDH, CDK5RAP1, LOC134145, NUP188*, and one unannotated transcript (clone IMAGE: 3839141; Fig. 6*B*). Among these six genes selected, *FOXM1* mRNA levels were found to be significantly elevated in clinical cases of lung cancer and showed good concordance with expression levels of *NMU* and two receptors, *GHSR1b* and *NTSR1* (Fig. 6*C*). To validate the induction of the *FOXM1* expression by the NMU ligand-receptor signaling, we cultured LC319 cells expressing GHSR1b and NTSR1 in the presence of NMU-25 or BSA (control) at final concentrations of 25 μmol/L in the culture media, and confirmed an enhanced expression of *FOXM1* in the NMU-treated cells (Fig. 6*D*). Furthermore, we did immunohistochemical analysis of NSCLCs with anti-FOXM1 polyclonal antibodies using tissue microarrays. Of the 325 cases of NSCLC available for this assay, FOXM1 staining was positive for 230 (70.8%; Supplementary Fig. S6*A*). The expression pattern of FOXM1 was significantly concordant with NMU expression in these tumors ($\chi^2 = 68$; $P < 0.0001$). We found that patients with NSCLC with FOXM1-positive tumors showed shorter survival times than patients whose tumors were negative for FOXM1 ($P = 0.0495$ by the log-rank test; Supplementary Fig. S6*B*). These results independently show that NMU, by the interaction with GHSR1b/NTSR1 heterodimer and subsequent activation of its downstream targets, such as *FOXM1*, could significantly affect the growth and malignant nature of lung cancer cells.

Discussion

Recent acceleration in the identification and characterization of novel molecular targets for cancer therapy has stimulated considerable interest in the development of new types of anticancer agents (3). Molecular-targeted drugs are expected to be highly specific to malignant cells, with minimal risk of adverse effects due to their well-defined mechanisms of action. As a promising strategy to identify such molecules, we combined the power of genome-wide expression analysis with high-throughput screening of loss-of-function effects by means of the RNAi technique. In addition, we used tissue microarrays to analyze hundreds of archived clinical samples for validation of the potential target proteins. Using this approach, we have shown here that *NMU* and its cancer-specific receptors, as well as its target genes,

are frequently overexpressed in clinical samples of lung cancer and in cell lines, and that those gene products play indispensable roles in the growth and progression of lung cancer cells.

A COOH-terminal asparaginamide structure and the COOH-terminal heptapeptide core of NMU protein are essential for its contractile activity in smooth muscle cells (30). Recent studies have indicated that NMU acts at the hypothalamic level to inhibit food intake; therefore, this protein might be a physiologic regulator of feeding and body weight (18, 31, 32). NMU was also expressed in several types of human tumors (33–35), but no reports have thus far suggested the involvement of NMU overexpression in pulmonary carcinogenesis, and its precise biological function in cancer cells have never been clarified.

Our treatment of NSCLC cells with specific siRNA to reduce the expression of *NMU* resulted in growth suppression. We also found other evidence supporting the significance of this pathway in carcinogenesis; e.g., the addition of NMU into the medium promoted the growth of COS-7 cells in a dose-dependent manner. The expression of NMU also resulted in the significant promotion of cell growth and invasion in *in vitro* assays. Moreover, clinicopathologic evidence obtained through our tissue microarray experiments showed that NSCLC patients with tumors expressing NMU showed shorter cancer-specific survival periods than those with negative NMU expression. The results obtained by *in vitro* and *in vivo* assays strongly suggested that overexpressed NMU is likely to be an important growth factor and might be associated with cancer cell growth and invasion, functioning in an autocrine manner, and that screening molecules targeting the NMU receptor growth-promoting pathway should be a promising therapeutic approach for treating lung cancers. Because NMU is a secreted protein and most of the clinical NSCLC samples used for our analysis were at an early and operable stage, NMU might also serve as a biomarker for diagnosis of early stage lung cancer, as well as an indicator for a highly malignant phenotype of lung cancer cells, in combination with fiberscopic transbronchial biopsy or blood tests.

NMU was already known to interact with at least two receptors, NMU1R (FM3/GPR66) and NMU2R (FM4), each of which has seven predicted α-helical transmembrane domains containing highly conserved motifs, as do other members of the rhodopsin GPCR family (17–19). The results presented here, however, indicated that these two known receptors were not the targets for the autocrine NMU-signaling pathway in NSCLCs; instead, the *GHSR1b* and

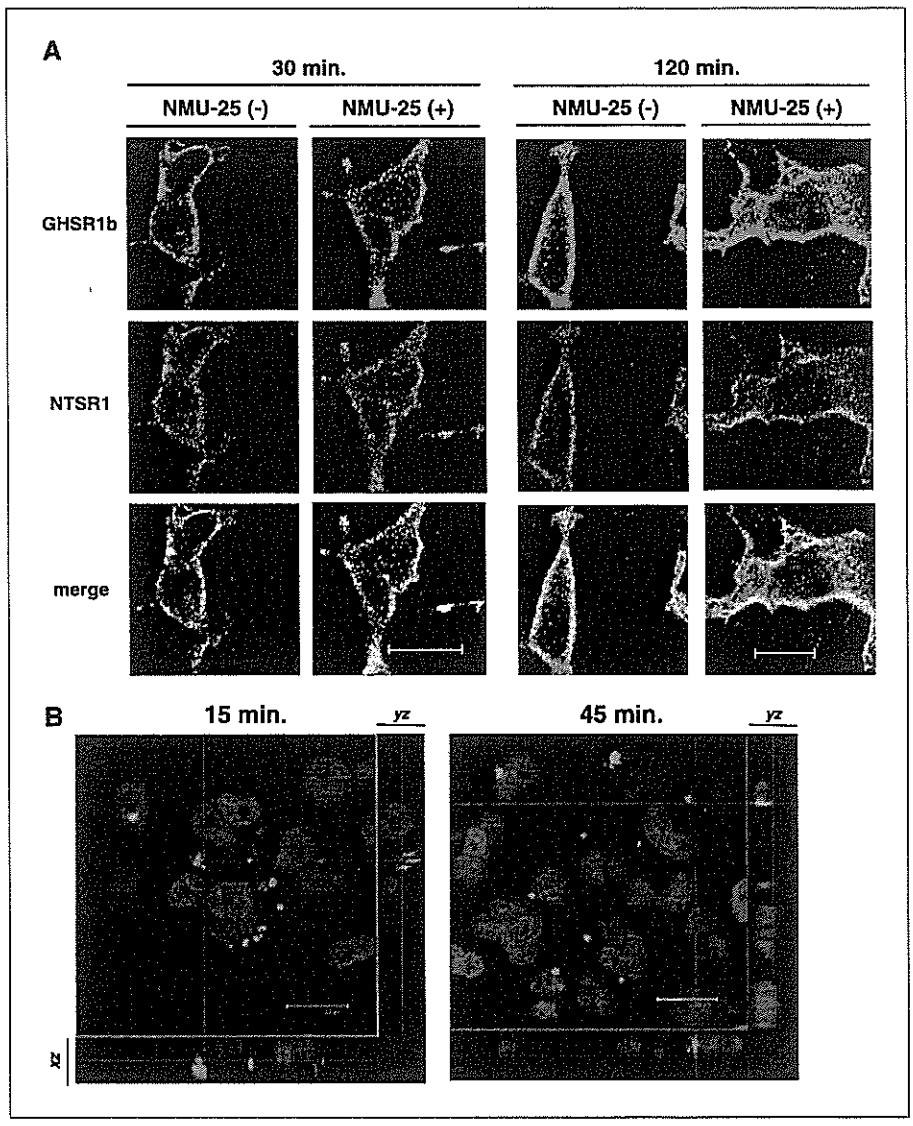

Figure 5. Characterization of GHSR1b/NTSR1 heterodimers and their internalization as cognate receptors for NMU. *A*, internalization of GHSR1b/NTSR1 protein induced by NMU-25. COS-7 cells transiently expressing both GHSR1b and NTSR1 were exposed to NMU-25 (10 μmol/L) for 30 minutes (*left*) or 120 minutes (*right*). COS-7 cells without exposure to the NMU-25 treatment served as controls. Cells were subsequently fixed and stained using secondary antibodies conjugated to Alexa Fluor 488–labeled anti-GHSR antibody or Alexa Fluor 594–labeled anti-NTSR1 antibody. Subcellular distribution of the two receptor proteins was examined by confocal microscopy. *Bottom*, LC319 cells expressing both endogenous GHSR1b and NTSR1 were exposed to NMU-25 (10 μmol/L) for 30 minutes (*left*) or 120 minutes (*right*). *B*, internalization of NMU-25-Alexa 594 in LC319 cells. The cells were incubated with 35 μmol/L of NMU-25-Alexa 594 for 15 minutes (*left*) or 45 minutes (*right*) at 37°C, and subsequently washed and fixed. *Red*, NMU-25-Alexa 594; *blue*, cell nuclei (with DAPI). The *xz*- and *yz*-projections proved that the ligands were localized within the cells. *Dotted lines*, where the *xz*- and *yz*-projections were taken.

NTSR1 heterodimer was implied to be the possible targets for the growth-promoting effect of NMU in lung tumors. GHSR is a known receptor of GHRL, a recently identified 28–amino acid peptide capable of stimulating the release of pituitary growth hormone and appetite in humans (23, 36, 37). Of the two transcripts known to be receptors for GHRL, GHSR1a and GHSR1b, we detected overexpression of only *GHSR1b* in NSCLC tissues and cell lines. In NSCLC, GHRL was not significantly expressed in the cell lines examined (Fig. 4*A*), therefore, we suspected that GHSR1b could have a growth-promoting function in lung tumors through binding to NMU, but not to GHRL. Interestingly, it was reported that *GHRL* and *GHSR1b*, but not *GHSR1a* genes were overexpressed in the erythroleukemic HEL cells, whose proliferation was regulated by des-acyl GHRL in an autocrine manner (38). NTSR1 is one of three receptors of NTS, a brain and gastrointestinal peptide that fulfills many central and peripheral functions (24). NTS modulates the transmission of dopamine and secretion of pituitary hormones, and exerts hypothermic and analgesic effects in the brain, whereas it functions as a peripheral hormone in the digestive tract and cardiovascular system. Others have reported that NTS is produced and secreted in several human cancers, including SCLCs (24). We detected the expression of *NTS* in 4 of the 15 NSCLC cell lines we

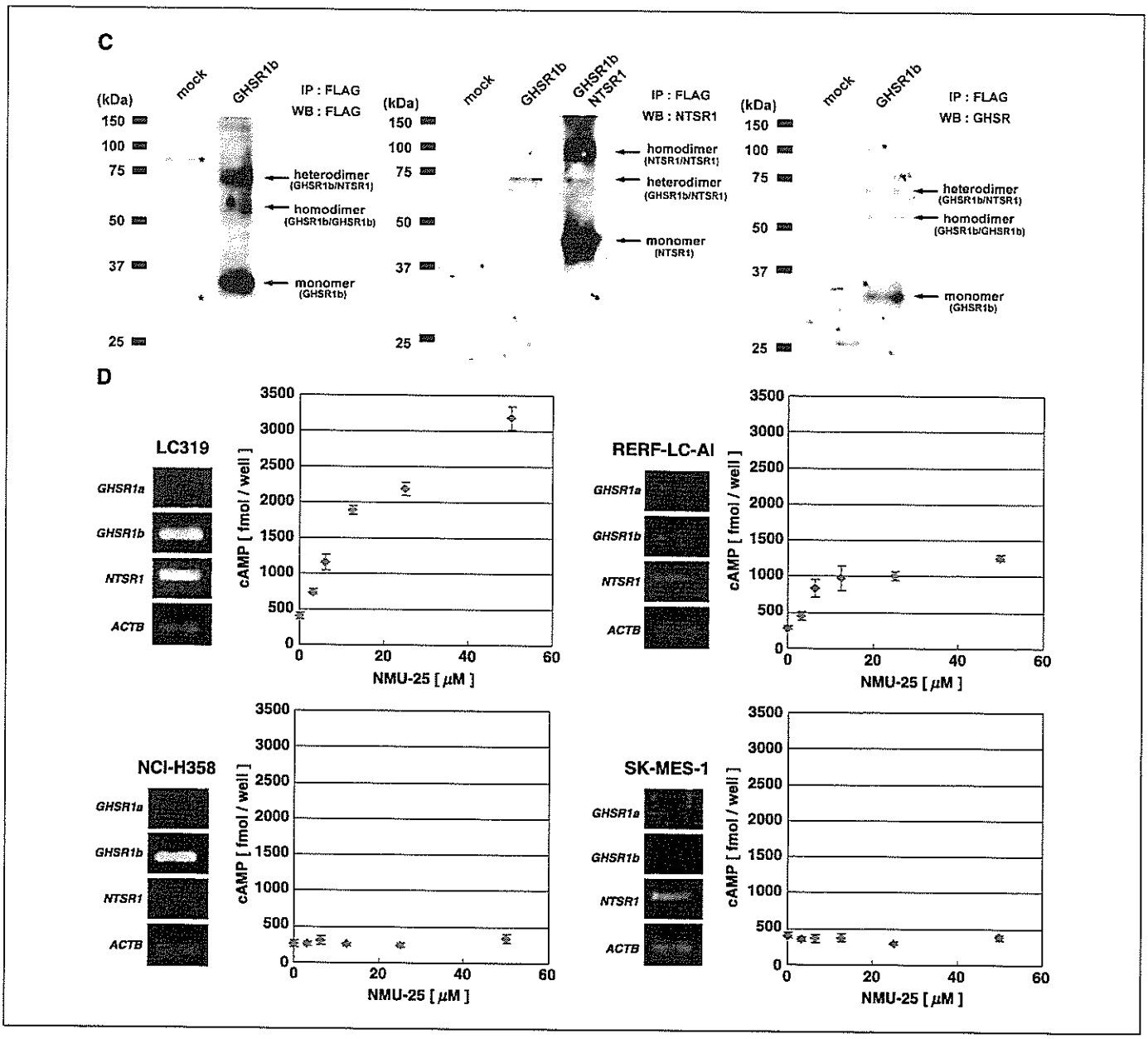

Figure 5 *Continued. C,* immunoprecipitation of cell lysates from COS-7 cells transiently expressed FLAG-tagged GHSR1b, and ones coexpressed both FLAG-tagged GHSR1b and NTSR1. The proteins immunoprecipitated by anti-FLAG antibody were subjected to SDS-PAGE and immunoblotted with anti-FLAG antibody (*left*), with anti-NTSR1 antibody (*middle*), or with anti-GHSR antibody (*right*). *Arrows,* monomers, heterodimers, and homodimers of the receptors. The molecular weight (kDa) markers are indicated on the left side of individual panels; *, nonspecific immunoreactive protein band detected by anti-FLAG antibody. *D,* relationship between the expression levels of GHSR1b/NTSR1 and intracellular cAMP production by NMU-25 in lung cancer cell lines. The expression levels of receptors in LC319, RERF-LC-AI, NCI-H358, and SK-MES-1 cells were detected by semiquantitative RT-PCR analysis. Dose-response curves of intracellular cAMP production by NMU-25 treatment (3-50 μmol/L) in individual cell lines are shown. All experiments were done in triplicate.

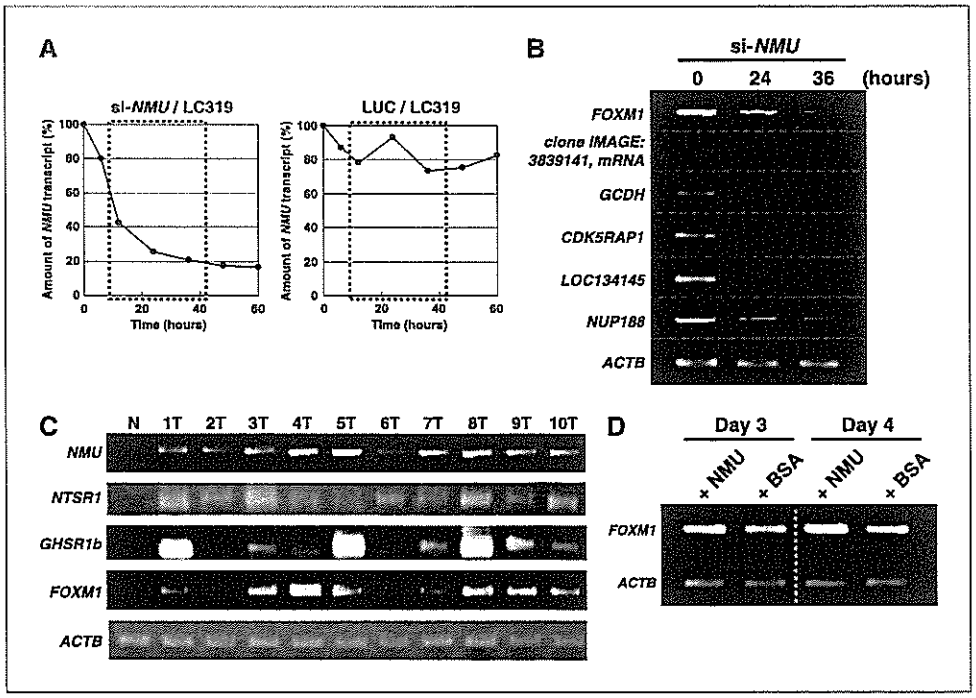

Figure 6. Identification of candidate downstream genes of the NMU signaling. *A*, time-dependent reduction of the *NMU* gene expression monitored by semiquantitative RT-PCR experiments of the mRNAs from LC319 cells treated with si-*NMU*, using *NMU*-specific primers. We prepared appropriate dilutions of each single-stranded cDNA prepared from mRNAs of LC319 cells at several time points. The β-actin (*ACTB*) expression was used as a quantitative control. Densitometric intensity of PCR product was quantified by image analysis software (Quantity One; Bio-Rad, Hercules, CA). *B*, time-dependent reduction of expression levels for possible target genes in the NMU signaling pathway was confirmed by semiquantitative RT-PCR experiments of mRNAs prepared from LC319 cells that were treated with si-*NMU*. Individual gene-specific primers were used for PCR amplification. *C*, expression of *NMU*, *NTSR1*, *GHSR1b*, and *FOXM1* in clinical NSCLC samples (*T*, lung tumor; *N*, normal lung tissue), examined by semiquantitative RT-PCR. *D*, induction of *FOXM1* expression in LC319 cells incubated with NMU-25, detected by semiquantitative RT-PCR using mRNAs prepared from LC319 cells treated with NMU-25 or BSA (as control; 25 μmol/L).

examined (Fig. 4*A*), but the expression pattern of *NTS* was not necessarily concordant with that of *NMU* or *NTSR1*. Therefore, we assume that NTS might contribute to the growth of NSCLC through NTSR1 or other receptor(s) in a small subset of NSCLCs.

In our experiments, the majority of the cancer cell lines and clinical NSCLCs that expressed NMU also expressed GHSR1b and NTSR1, indicating that these ligand-receptor interactions were likely to be involved in a pathway that is central to the growth-promoting activity of NMU in NSCLCs. *GHSR* and *NTSR1* were also expressed in COS-7 cells used to examine the growth and invasion effect of NMU; the data strongly supported the importance of these two receptors for oncogenesis. Our experiments further revealed that NMU-25 functionally bound to these receptors on the cell surface of NSCLC cells and subsequently induced the production of a second messenger, cAMP. We also showed that treatment of NSCLC cells with siRNAs for *GHSR* or *NTSR1* reduced the expression of these receptors and resulted in cancer growth inhibition. Elevated cAMP levels were generally observed via activation of adenylate cyclase, which activated protein kinase A (PKA). It was reported that GHRL did not displace ^{125}I-labeled rat NMU binding to NMU1R-expressing cells when tested at concentrations up to 10 mmol/L (39). However, GHRL or NTS competitively inhibited NMU-induced cAMP production in NSCLC cells.[8] Moreover, we provide biochemical and physiologic evidence for the internalization and heterodimerization of the two neuropeptide GPCRs, GHSR1b and NTSR1 (Fig. 5*A*; Supplementary Fig. S5). These results independently suggest that NMU stimulates NSCLC cell proliferation by a pathway through the GHSR1b-NTSR1 heterodimer whose function is quite different from the two known NMU-receptors, NMU1R and NMU2R. Heterodimerization has been shown to contribute to both ligand-binding affinity and signaling efficacy of GPCRs (40, 41). Heterodimers can be formed by receptors for various ligands/transmitters; for example, GPCRs for angiotensin and bradykinin (42), or those for opioid and adrenergic ligands (43). Moreover, it has been reported that coexpression of GHSR1a and GHSR1b resulted in an attenuation of the signaling capability of GHSR1a, suggesting that GHSR1b possibly interacted with GHSR1a through receptor heterodimerization (44). Based on the fact that GHSR1b exhibits no function towards GHRL (45), heterodimerization of GHSR1a and GHSR1b might in fact be a common feature for GHSR. The combination of our data with previous reports suggests that binding of NMU to GHSR1b/NTSR1 heterodimer, which cooperated with G proteins of the G_s subfamily, leads to the activation of adenylate cyclase, accumulation of intracellular cAMP, and activation of cAMP-dependent protein kinase (PKA), and that the subsequent release of catalytic subunits of PKA (C) from the regulatory subunits (R) activates downstream target genes, thus, finally resulting in the activation of growth-promoting pathways.

Microarray data of LC319 cells treated with siRNA for *NMU* suggests that the NMU signaling pathway could affect the growth promotion of lung cancer cells by transactivating a set of downstream genes. We provided evidence that the FOXM1 transcription factor is one of the downstream targets in the NMU signaling pathway. In our tissue microarray experiments, we observed that the expression pattern of FOXM1 was significantly concordant with that of NMU in the same set of tumors, and that lung cancer patients with FOXM1-positive tumors showed shorter survival periods than patients with FOXM1-negative tumors, thus, independently confirming the effect of NMU-FOXM1 signaling on the promotion of the malignant nature of lung cancer cells. FOXM1 was known to be overexpressed in several types of human cancers (46–48). We also confirmed that treatment of NSCLC cells with specific siRNA to reduce the expression of *FOXM1* resulted in growth suppression.[8] To predict the transcriptional regulation of the *FOXM1* gene by cAMP-response element (CRE)–binding protein, we also screened the CRE-like sequence within a 1-kb upstream region of the putative transcription start sequence using the computer prediction program and found that the region

[8] Unpublished data.

contains three CRE-like elements (data not shown). Moreover, it should be noted that the luciferase reporter gene assay suggested that two of the CRE-like sequences are essential for effective augmentation of *FOXM1* promoter activity following NMU stimulation.[8] We speculate that CRE-binding proteins phosphorylated by PKA might be directly responsible for the regulation of *FOXM1* expression. Previous reports suggested that some cyclin genes are possible transcription targets of FOXM1 transcription factor and that FOXM1 controls the transcription network of genes which are essential for cell division and exit from mitosis (29). In fact, we observed the activation of *CCNB1* and *CCNA2* in the majority of a series of clinical NSCLC we examined and its good concordance of the expression to *FOXM1* expression. These data indicate the possibility that the NMU-FOXM1 pathway is finally linked to cyclin-dependent pathways.

In summary, we have shown that NMU and the recently identified heterodimerization of GHSR1b and NTSR1 are likely to play an essential role for an autocrine growth-promoting pathway in NSCLCs by modulating the transcription of downstream target genes including *FOXM1*. The data reported here strongly imply the possibility of designing new anticancer drugs, specific for lung cancer, that target the NMU-GHSR1b/NTSR1 pathway as well as the development of novel diagnostic/prognostic markers for lung cancer.

Acknowledgments

Received 4/18/2006; revised 7/24/2006; accepted 8/4/2006.

Grant support: "Research for the Future" Program Grant of The Japan Society for the Promotion of Science (no. 00L01402) to Y. Nakamura.

The costs of publication of this article were defrayed in part by the payment of page charges. This article must therefore be hereby marked *advertisement* in accordance with 18 U.S.C. Section 1734 solely to indicate this fact.

References

1. Greenlee RT, Hill-Harmon MB, Murray T, Thun M. Cancer statistics. CA Cancer J Clin 2001;51:15–36.
2. Sozzi G. Molecular biology of lung cancer. Eur J Cancer 2001;37:63–73.
3. Schiller JH, Harrington D, Belani CP, et al. Comparison of four chemotherapy regimens for advanced non-small-cell lung cancer. N Engl J Med 2001;346:92–8.
4. Kikuchi T, Daigo Y, Katagiri T, et al. Expression profiles of non-small cell lung cancers on cDNA microarrays: identification of genes for prediction of lymph-node metastasis and sensitivity to anti-cancer drugs. Oncogene 2003;22:2192–205.
5. Kakiuchi S, Daigo Y, Ishikawa N, et al. Prediction of sensitivity of advanced non-small cell lung cancers to gefitinib (Iressa, ZD1839). Hum Mol Genet 2004;13:3029–43.
6. Suzuki C, Daigo Y, Kikuchi T, Katagiri T, Nakamura Y. Identification of COX17 as a therapeutic target for non-small cell lung cancer. Cancer Res 2003;63:7038–41.
7. Suzuki C, Daigo Y, Ishikawa N, et al. ANLN plays a critical role in human lung carcinogenesis through activation of RHOA and by involvement in PI3K/AKT pathway. Cancer Res 2005;65:11314–25.
8. Ishikawa N, Daigo Y, Yasui W, et al. ADAM8 as a novel serological and histochemical marker for lung cancer. Clin Cancer Res 2004;10:8363–70.
9. Ishikawa N, Daigo Y, Takano A, et al. Increases of amphiregulin and transforming growth factor-α in serum as predictors of poor response to gefitinib among patients with advanced non-small cell lung cancers. Cancer Res 2005;65:9176–84.
10. Kato T, Daigo Y, Hayama S, et al. A novel human tRNA-dihydrouridine synthase involved in pulmonary carcinogenesis. Cancer Res 2005;65:5638–46.
11. Furukawa C, Daigo Y, Ishikawa N, et al. PKP3 oncogene as prognostic marker and therapeutic target for lung cancer. Cancer Res 2005;65:7102–10.
12. Minamino N, Kangawa K, Matsuo H. Neuromedin U-8 and U-25: novel uterus stimulating and hypertensive peptides identified in porcine spinal cord. Biochem Biophys Res Commun 1985;130:1078–85.
13. Domin J, Ghatei MA, Chohan P, Bloom SR. Characterization of neuromedin U-like immunoreactivity in rat, porcine, guinea-pig and human tissue extracts using a specific radioimmunoassay. Biochem Biophys Res Commun 1986;140:1127–34.
14. Domin J, Yiangou YG, Spokes RA, et al. The distribution, purification, and pharmacological action of an amphibian neuromedin U. J Biol Chem 1989;264:20881–5.
15. Kage R, O'Harte F, Thim L, Conlon JM. Rabbit neuromedin U-25: lack of conservation of a posttranslational processing site. Regul Pept 1991;33:191–8.
16. Austin C, Oka M, Nandha KA, et al. Distribution and developmental pattern of neuromedin U expression in the rat gastrointestinal tract. J Mol Endocrinol 1994;12:257–63.
17. Fujii R, Hosoya M, Fukusumi S, et al. Identification of neuromedin U as the cognate ligand of the orphan G protein-coupled receptor FM-3. J Biol Chem 2000;275:21068–74.
18. Howard AD, Wang R, Pong SS, et al. Identification of receptors for neuromedin U and its role in feeding. Nature 2000;406:70–4.
19. Funes S, Hedrick JA, Yang S, et al. Cloning and characterization of murine neuromedin U receptors. Peptides 2002;23:1607–15.
20. Chin SF, Daigo Y, Huang HE, et al. A simple and reliable pretreatment protocol facilitates fluorescent *in situ* hybridisation on tissue microarrays of paraffin wax embedded tumour samples. Mol Pathol 2003;56:275–9.
21. Callagy G, Cattaneo E, Daigo Y, et al. Molecular classification of breast carcinomas using tissue microarrays. Diagn Mol Pathol 2003;12:27–34.
22. Kohonen T. The self-organizing map. Proc IEEE 1990;78:1464–80.
23. Kojima M, Hosoda H, Date Y, Nakazato M, Matsuo H, Kangawa K. Ghrelin is a growth-hormone-releasing acylated peptide from stomach. Nature 1999;402:656–60.
24. Heasley LE. Autocrine and paracrine signaling through neuropeptide receptors in human cancer. Oncogene 2001;20:1563–9.
25. Bohm SK, Grady EF, Bunnett NW. Regulatory mechanisms that modulate signalling by G-protein-coupled receptors. Biochem J 1997;322:1–18.
26. Koenig JA, Edwardson JM. Endocytosis and recycling of G protein-coupled receptors. Trends Pharmacol Sci 1997;18:276–87.
27. Ghinea N, Vu Hai MT, Groyer-Picard MT, Houllier A, Schoevaert D, Milgrom E. Pathways of internalization of the hCG/LH receptor: immunoelectron microscopic studies in Leydig cells and transfected L-cells. J Cell Biol 1992;118:1347–58.
28. Vandenbulcke F, Nouel D, Vincent JP, Mazella J, Beaudet A. Ligand-induced internalization of neurotensin in transfected COS-7 cells: differential intracellular trafficking of ligand and receptor. J Cell Sci 2000;113:2963–75.
29. Faure MP, Alonso A, Nouel D, et al. Somatodendritic internalization and perinuclear targeting of neurotensin in the mammalian brain. J Neurosci 1995;15:4140–7.
30. Austin C, Nandha KA, Meleagros L, Bloom SR. Cloning and characterization of the cDNA encoding the human neuromedin U precursor: NMU expression in the human gastrointenstinal tract. J Mol Endocrinol 1995;14:157–69.
31. Ivanov TR, Lawrence CB, Stanley PJ, Luckman SM. Evaluation of neuromedin U actions in energy homeostasis and pituitary function. Endocrinology 2002;143:3813–21.
32. Hanada R, Teranishi H, Pearson JT, et al. Neuromedin U has a novel anorexigenic effect independent of the leptin signaling pathway. Nat Med 2004;10:1067–73.
33. Steel JH, Van Noorden S, Ballesta J, et al. Localization of 7B2, neuromedin B, and neuromedin U in specific cell types of rat, mouse, and human pituitary, in rat hypothalamus, and in 30 human pituitary and extrapituitary tumors. Endocrinology 1988;122:270–82.
34. Shetzline SE, Rallapalli R, Dowd KJ, et al. Neuromedin U: a Myb-regulated autocrine growth factor for human myeloid leukemias. Blood 2004;104:1833–40.
35. Euer NI, Kaul S, Deissler H, Mobus VJ, Zeillinger R, Weidle UH. Identification of L1CAM, Jagged2 and Neuromedin U as ovarian cancer-associated antigens. Oncol Rep 2005;13:375–87.
36. Kim K, Arai K, Sanno N, Osamura RY, Teramoto A, Shibasaki T. Ghrelin and growth hormone (GH) secretagogue receptor (GHSR) mRNA expression in human pituitary adenomas. Clin Endocrinol (Oxf) 2001;54:759–68.
37. Lambert PD, Anderson KD, Sleeman MW, et al. Ciliary neurotrophic factor activates leptin-like pathways and reduces body fat, without cachexia or rebound weight gain, even in leptin-resistant obesity. Proc Natl Acad Sci U S A 2001;98:4652–7.
38. De Vriese C, Gregoire F, De Neef P, Robberecht P, Delporte C. Ghrelin is produced by the human erythroleukemic HEL cell line and involved in an autocrine pathway leading to cell proliferation. Endocrinology 2005;146:1514–22.
39. Kojima M, Haruno R, Nakazato M, et al. Purification and identification of neuromedin U as an endogenous ligand for an orphan receptor GPR66 (FM3). Biochem Biophys Res Commun 2000;276:435–8.
40. Bouvier M. Oligomerization of G-protein-coupled transmitter receptors. Nat Rev Neurosci 2001;2:274–86.
41. Devi LA. Heterodimerization of G-protein-coupled receptors: pharmacology, signaling and trafficking. Trends Pharmacol Sci 2001;22:532–7.
42. AbdAlla S, Lother H, Quitterer U. AT1-receptor heterodimers show enhanced G-protein activation and altered receptor sequestration. Nature 2000;407:94–8.
43. Rocheville M, Lange DC, Kumar U, Patel SC, Patel RC, Patel YC. Receptors for dopamine and somatostatin: formation of hetero-oligomers with enhanced functional activity. Science 2000;288:154–7.
44. Chan CB, Cheng CH. Identification and functional characterization of two alternatively spliced growth hormone secretagogue receptor transcripts from the pituitary of black seabream *Acanthopagrus schlegeli*. Mol Cell Endocrinol 2004;214:81–95.
45. Howard AD, Feighner SD, Cully DF, et al. A receptor in pituitary and hypothalamus that functions in growth hormone release. Science 1996;273:974–7.
46. Teh MT, Wong ST, Neill GW, Ghali LR, Philpott MP, Quinn AG. FOXM1 is a downstream target of Gli1 in basal cell carcinomas. Cancer Res 2002;62:4773–80.
47. van den Boom J, Wolter M, Kuick R, et al. Characterization of gene expression profiles associated with glioma progression using oligonucleotide-based microarray analysis and real-time reverse transcription-polymerase chain reaction. Am J Pathol 2003;163:1033–43.
48. Kalinichenko VV, Major ML, Wang X, et al. Foxm1b transcription factor is essential for development of hepatocellular carcinomas and is negatively regulated by the p19ARF tumor suppressor. Genes Dev 2004;18:830–50.

Original Paper

Pathobiology

Pathobiology 2006;73:93–97
DOI: 10.1159/000094493

Received: January 24, 2006
Accepted: April 12, 2006

Nuclear and Mitochondrial DNA Microsatellite Instability in Gastrointestinal Stromal Tumors

K. Kose[a] T. Hiyama[d] S. Tanaka[c] M. Yoshihara[d] W. Yasui[b] K. Chayama[a]

[a]Department of Medicine and Molecular Science, Division of Frontier Medical Science, [b]Department of Molecular Pathology, Division of Molecular Medical Science, Programs for Biomedical Research, Graduate School of Biomedical Sciences, Hiroshima University, [c]Department of Endoscopy, Hiroshima University Hospital, Hiroshima, and [d]Health Service Center, Hiroshima University, Higashihiroshima, Japan

Key Words

Gastrointestinal stromal tumor · Nuclear microsatellite instability · Mitochondrial microsatellite instability · BAT26 · D310

Abstract

Objective: Gastrointestinal stromal tumors (GISTs) are the most common mesenchymal tumors of the digestive tract. Nuclear (nMSI) and mitochondrial microsatellite instability (mtMSI) play important roles in tumorigenesis in various organs. The aim of this study was to evaluate the role of nMSI and mtMSI in GISTs. ***Methods:*** Samples from 74 mesenchymal tumors were collected. nMSI and mtMSI were examined by microsatellite assay at BAT26 and D310 mononucleotide repeats in mtDNA, respectively. We compared nMSI, mtMSI and clinicopathologic features, including patient age and sex, tumor location, tumor size, presence of tumor ulceration and presence of distant metastasis, for 51 GISTs for which these data were available. ***Results:*** nMSI and mtMSI were detected in 3 (5%) and 10 (16%) of the 62 GISTs, respectively. There was no significant relationship between nMSI, mtMSI and clinicopathologic features. ***Conclusion:*** These results suggest that mtMSI may play a role, but that nMSI may play little role in the development of GISTs.

Introduction

Gastrointestinal stromal tumors (GISTs), previously classified as smooth muscle tumors, are the most common primary mesenchymal tumors of the gastrointestinal tract [1]. GISTs represent a spectrum of tumors including benign and malignant variants. The immunophenotypic characteristics and genetic profiles of GISTs have clearly distinguished them as a tumor entity separate from other mesenchymal tumors. GISTs are usually positive for the expression of CD34 and c-kit oncoprotein, a transmembrane tyrosine kinase receptor for stem cell factor [2]. Recent studies have shown that mutations of the c-*kit* gene resulting in constitutive activation of the tyrosine kinase play a significant role in tumor pathogenesis [3, 4]. Although c-*kit* mutation was identified in 60–90% of tumors [2, 5], some other molecular alterations may be associated with the development and progression of GISTs [6–9].

Several types of hereditary and sporadic human tumors show high rates of spontaneous mutations due to malfunction of one or more of the mismatch repair genes [10]. Disrupted function of mismatch repair genes manifests itself as nuclear microsatellite instability (nMSI). nMSI has been reported in 80–95% of hereditary nonpolyposis colorectal cancers, in 10–30% of sporadic colorec-

KARGER

Fax +41 61 306 12 34
E-Mail karger@karger.ch
www.karger.com

1015–2008/06/0732–0093$23.50/0

Accessible online at:
www.karger.com/pat

Dr. Shinji Tanaka
Department of Endoscopy, Hiroshima University Hospital
1-2-3 Kasumi, Minami-ku
Hiroshima 734-8551 (Japan)
Tel. +81 82 257 5193, Fax +81 82 257 5194, E-Mail colon@hiroshima-u.ac.jp

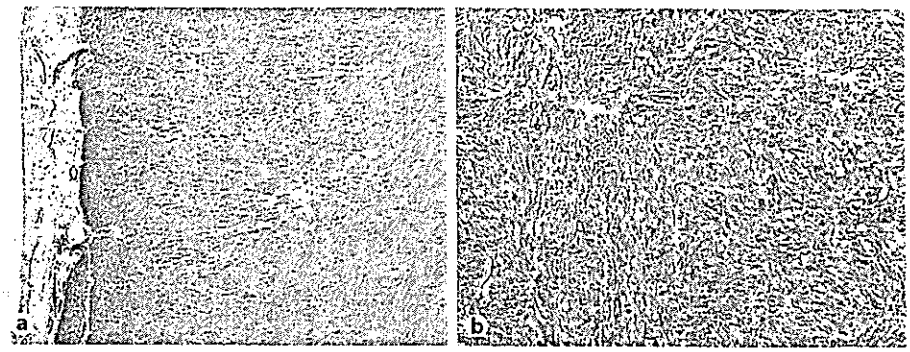

Fig. 1. Representative examples of immunohistochemical staining for KIT. Positive staining was observed. HE. **a** ×40. **b** ×200.

tal cancers and in 15–39% of sporadic gastric cancers [10]. Eukaryote cells not only have a nuclear genome but also cytoplasmic genomes that are compartmentalized in the mitochondria. Mitochcondrial microsatellite instability (mtMSI) is also reported in several types of tumors [11]. However, there are few studies on nMSI and mtMSI in GISTs. We therefore analyzed the nMSI and mtMSI in these tumors in the present study.

Materials and Methods

Tissue Samples

At the Hiroshima University Hospital 74 mesenchymal tumors of the stomach were collected during the period of 1980 through 2000. The mesenchymal tumors were identified as GISTs on the basis of positive immunohistochemical staining for KIT and/or CD34 (fig. 1). With this criterion 62 of the 74 tumors (84%) were identified as GISTs. For each case tumorous and normal tissues were obtained. Clinicopathologic data, including age, sex, tumor location, tumor size, presence of tumor ulceration and presence of distant metastasis, were obtained for 51 of the patients. This study was approved by the local ethics committee (No. I-RIN-HI-45).

Histologic Examination

Four-micron-thick sections were prepared from formalin-fixed, paraffin-embedded specimens. The sections were stained with hematoxylin and eosin (HE) for histologic examination.

DNA Extraction

Ten-micron-thick tissue sections were placed onto glass slides and stained with HE. The sections were then dehydrated in graded ethanol and dried without a cover glass. Tumorous and normal tissues on the slides were scraped up separately with sterile needles. DNA was extracted from the tissues with 20 μl of extraction buffer (100 mM of Tris-HCl, 2 mM of EDTA, pH 8.0, and 400 μl/ml of proteinase K) at 50°C overnight. The samples in tubes were boiled for 7 min to inactivate proteinase K, and 2 μl of aliquots were used for each polymerase chain reaction (PCR) amplification.

Analysis of nMSI

Each tumor was evaluated for nMSI by microsatellite assay with BAT26. The microsatellite assay was performed as described elsewhere [12, 13]. Briefly each 15 μl of reaction mixture containing 10–20 ng of genomic DNA, 6.7 mM of Tris-HCl (pH 8.8), 6.7 mM of EDTA, 6.7 mM of $MgCl_2$, 0.33 μM of labeled primer with [γ-^{32}P]dATP, 0.175 μM unlabeled primer, 1.5 mM of each deoxynucleotide triphosphate and 0.75 U of AmpliTaq Gold DNA polymerase (Perkin-Elmer, Branchburg, N.J., USA) was amplified for 40 cycles as follows: denaturation at 94°C for 30 s, annealing at 55°C for 30 s and strand elongation at 72°C for 30 s. The PCR products were electrophoresed on 6% polyacrylamide-8 M urea-32% formamide gels and autoradiographed overnight at –80°C on Fuji RX film. Tumors with shifted bands at the BAT26 were classified as nMSI [14].

Analysis of mtMSI

A 109-bp fragment containing the D310 repeat of mitochondrial DNA (mtDNA; D-loop region) was amplified [15]. The primer sequences were as follows: 5′-ACAATTGAATGTCTGCACAGCCACTT-3′ for the sense primer and 5′-GGCAGAGATGTGTTTAAGTGCTG-3′ for the antisense primer. Microsatellite assays were performed. Tumors with shifted bands at the D310 repeat were classified as mtMSI [11].

Statistical Analysis

Fisher's exact probability test was used to identify the relationship between D310 mutation and clinicopathologic features. A p value <0.05 was significant.

Results

Clinicopathologic Features of GISTs

Clinicopathologic data including age, sex, tumor location, tumor size, presence of tumor ulceration and presence of distant metastasis were available for 51 cases. All of the 51 GISTs analyzed were located in the stomach and obtained during surgical resection. The male-to-female ratio of the patients was 31:20. The mean age of these patients was 59.0 years (range 20–81). The mean tumor di-

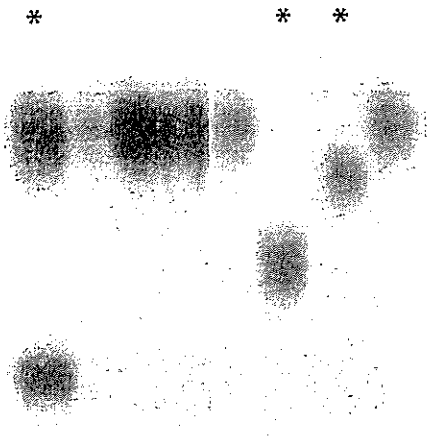

Fig. 2. Representative examples of nMSI. Asterisks indicate a 1-bp deletion of the BAT26 locus.

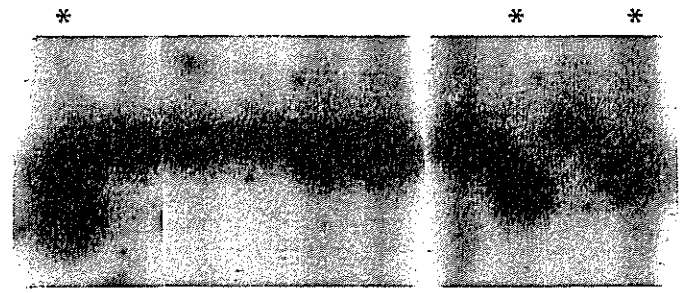

Fig. 3. Representative examples of mtMSI. Asterisks indicate a 1-bp deletion of the D310 mononucleotide repeat.

ameter was 52.1 mm (range 15–200). Thirty-four GISTs (67%) were located in the upper and 17 (33%) in the lower stomach. Forty-two cases (82%) were negative for distant metastasis, and 9 (18%) were positive. Fourteen cases (27%) showed ulceration of the tumor surface and 37 (73%) did not.

Analysis of nMSI

nMSI was detected in 3 of the 62 tumors (5%; fig. 2). Of the 3 positive tumors 1 (33%) showed deletions of 1 bp, 1 (33%) of 3 bp and 1 of 5 bp. We then compared nMSI with the clinicopathologic features in 51 tumors for which clinicopathologic data were available (table 1). No significant relationship was identified between nMSI and each clinicopathologic feature.

Analysis of mtMSI

mtMSI was detected in 10 of the 62 tumors (16%; fig. 3). Of the 10 positive tumors 6 (60%) showed insertions of 1bp, the remaining 4 (40%) deletions of 1bp. We then compared mtMSI with the clinicopathologic features in the 51 tumors for which clinicopathologic data were available (table 2). No significant relationships were identified between mtMSI and each clinicopathologic feature.

Relationship between nMSI and mtMSI

We then examined the relationship between nMSI and mtMSI (table 3). There was no significant relationship between nMSI and mtMSI in GISTs.

Table 1. nMSI in relation to clinicopathologic characteristics of GISTs

Characteristics	nMSI		Frequency of nMSI %	p value
	positive	negative		
Patient age, years				
<60	0	27	0	NS
≥ 60	2	22	8	
Patient sex				
Male	2	29	6	NS
Female	0	20	0	
Tumor location				
Upper	1	33	3	NS
Lower	1	16	6	
Tumor size (diameter), mm				
<50	1	32	3	NS
≥ 50	1	16	6	
Tumor ulceration				
Positive	1	13	7	NS
Negative	1	36	3	
Distant metastasis				
Positive	1	8	11	NS
Negative	1	41	2	

NS = Not significant.

Discussion

The molecular pathogenesis of GIST is not fully understood. Alterations in the mismatch repair genes (*hMLH1*, *hMSH2*, *hMSH6*, etc.) are responsible for colorectal, gastric and endometrial tumor formation [10, 11]. Disrupted function of mismatch repair genes manifests itself as nMSI. The cases are classified as having high-frequency MSI (2 or more of 5 microsatellite loci show instability), low-frequency MSI (only 1 of the loci shows instability)

Table 2. mtDNA mutation in relation to clinicopathologic characteristics of GISTs

Characteristics	mtMSI		Frequency of mtMSI %	p value
	positive	negative		
Patient age, years				
<60	4	23	15	NS
≥60	4	20	17	
Patient sex				
Male	7	24	23	NS
Female	1	19	5	
Tumor location				
Upper	5	29	15	NS
Lower	3	14	18	
Tumor size (diameter), mm				
<50	6	27	18	NS
≥50	2	16	11	
Tumor ulceration				
Positive	2	12	14	NS
Negative	6	31	16	
Distant metastasis				
Positive	1	8	11	NS
Negative	7	35	17	

NS = Not significant.

Table 3. Relationship between nMSI and mtMSI in GISTs

	mtMSI		p value
	positive	negative	
nMSI			
Positive	0	3	NS
Negative	8	40	

NS = Not significant.

and microsatellite stable (none of the loci show instability) [16]. As a single test of BAT26 can identify cases positive for high-frequency MSI [13], we evaluated nMSI with microsatellite assay at the BAT26 locus. There are only 2 studies on nMSI in GISTs [17, 18]. One study [18] showed that nMSI was detected in 27% of the tumors and another [17] that no nMSI was found. In the present study nMSI was detected in 4% of the tumors, and it showed that there is no significant relationship between nMSI and clinicopathologic features. These data suggest that nMSI may play little role in the development of GISTs.

The importance of mtDNA in apoptosis has been suggested in several studies[e.g. 19]. Cytochrome c is released from mitochondria, and this is inhibited by the presence of Bcl-2. Cytochrome c interacts with Apaf-1 and procaspase-9 and activates other caspases, leading to apoptosis. This process may be disrupted by mitochondrial dysfunction such as that occurring with mtMSI, and unlimited cell proliferation may result in affected tissues. Tan et al. [20] reported that 22 of 27 breast cancers (81%) had mtMSI. mtMSI was evaluated with alteration of the D-loop region in mtDNA. The region is known to be the start site for replication of the closed, circular mitochondrial genome [21]. Replication of mtDNA begins with the synthesis of the heavy strand with primer RNA, and the 3′ termini of primer RNA have been mapped to CSBs I–III [22]. The identification of alterations in this region indicates the necessity of further research into the mechanisms of late replication and processing of mtDNA in tumors. There have been no studies on mtMSI in GISTs; the present study is the first one. We detected mtMSI in 15% of GISTs, indicating that mtMSI may be involved in the pathogenesis of GISTs. We found no significant relationship between mtMSI and clinicopathologic features. These data suggest that mtMSI may play an important role in the development, but not in the progression of GISTs.

What is the relationship between nMSI and mtMSI, and what is the functional importance of these events for the evolution of cancer cells? Recently Habano et al. [23] reported the existence of an association between nMSI and mtMSI in gastric cancers. However, no such association was found by several other researchers [24, 25]. In addition to these studies no relationship between nMSI and mtMSI has been reported in colorectal, breast and hepatocellular carcinoma [26, 27]. We did not find any relationship between nMSI and mtMSI in GISTs in the present study. NMSI and mtMSI may be independent events in human carcinogenesis.

In conclusion our results suggest that mtMSI may play a role, but that nMSI plays little role in the development of GISTs.

Acknowledgment

We thank Ms. N. Kubota for her technical assistance.

References

1 Miettinen M, Lasota J: Gastrointestinal stromal tumors: definition, clinical, histological, immunohistochemical, and molecular genetic features and differential diagnosis. Virchows Arch 2001;438:1–12.

2 Rubin BP, Singer S, Tsao C, Duensing A, Lux ML, Ruiz R, Hibbard MK, Chen CJ, Xiao S, Tuveson DA, Demetri GD, Fletcher CD, Fletcher JA: KIT activation is a ubiquitous feature of gastrointestinal stromal tumors. Cancer Res 2001;61:8118–8121.

3 Hirota S, Isozaki K, Moriyama Y, Hashimoto K, Nishida T, Ishiguro S, Kawano K, Hanada M, Kurata A, Takeda M, Muhammad Tunio G, Matsuzawa Y, Kanakura Y, Shinomura Y, Kitamura Y: Gain-of-function mutations of c-kit in human gastrointestinal stromal tumors. Science 1998;279:577–580.

4 Nishida T, Hirota S, Taniguchi M, Hashimoto K, Isozaki K, Nakamura H, Hanakura Y, Tanaka T, Takabayashi A, Matsuda H, Kitamura Y: Familial gastrointestinal stromal tumors with germline mutation of the KIT gene. Nat Genet 1998;19:323–324.

5 Taniguchi M, Nishida T, Hirota S, Isozaki K, Ito T, Nomura T, Matsuda H, Kitamura Y: Effect of c-*kit* mutation on prognosis of gastrointestinal stromal tumors. Cancer Res 1999;59:4297–4300.

6 Yamashita K, Igarashi H, Kitayama Y, Ozawa T, Kiyose S, Konno H, Kazui T, Ishikawa S, Aburatani H, Tanioka F, Suzuki M, Sugimura H: Chromosomal numerical abnormality profiles of gastrointestinal stromal tumors. Jpn J Clin Oncol 2006;36:85–92.

7 Blair SL, Al-Refaie WB, Wang-Rodriguez J, Behling C, Ali MW, Moossa AR: Gastrointestinal stromal tumors express ras oncogene: a potential role for diagnosis and treatment. Arch Surg 2005;140:547–548.

8 Nishitani A, Hirota S, Nishida T, Isozaki K, Hashimoto K, Nakagomi N, Matsuda H: Differential expression of connexin 43 in gastrointestinal stromal tumours of gastric and small intestinal origin. J Pathol 2005;206:377–382.

9 Tornillo L, Duchini G, Carafa V, Lugli A, Dirnhofer S, Di Vizio D, Boscaino A, Russo R, Tapia C, Schneider-Stock R, Sauter G, Insabato L, Terracciano LM: Patterns of gene amplification in gastrointestinal stromal tumors (GIST). Lab Invest 2005;85:921–931.

10 Yuen ST, Chan TL, Ho JWC, Chan ASY, Chung LP, Lam PWY, Tse CW, Wyllie AH, Leung SY: Germline, somatic and epigenetic events underlying mismatch repair deficiency in colorectal and HNPCC-related cancer. Oncogene 2002;21:7585–7592.

11 Habano W, Nakamura S, Sugai T: Microsatellite instability in the mitochondrial DNA of colorectal carcinomas: evidence for mismatch repair systems in mitochondrial genome. Oncogene 1998;17:1931–1937.

12 Hiyama T, Yokozaki H, Shimamoto F, Haruma K, Yasui W, Kajiyama G, Tahara E: Frequent *p53* gene mutations in serrated adenomas of the colorectum. J Pathol 1998;186:131–139.

13 Miyoshi E, Haruma K, Hiyama T, Tanaka S, Yoshihara M, Shimamoto F, Chayama K: Microsatellite instability is a genetic marker for the development of multiple gastric cancers. Int J Cancer 2001;95:350–353.

14 Zhou XP, Hoang JM, Li YJ, Seruca R, Carneiro F, Sobrinho-Simoes M, Lothe RA, Gleeson CM, Russell SE, Muzeau F, Flejou JF, Hoang-Xuan K, Lidereau R, Thomas G, Hamelin R: Determination of the replication error phenotype in human tumors without the requirement for matching normal DNA by analysis of mononucleotide repeat microsatellites. Genes Chromosomes Cancer 1998;21:101–107.

15 Sanchez-Cespedes M, Parrella P, Nomoto S, Cohen D, Xiao Y, Esteller M, Jeronimo C, Jordan RC, Nicol T, Koch WM, Schoenberg M, Mazzarelli P, Fazio VM, Sidransky D: Identification of a mononucleotide repeat as a major target for mitochondrial DNA alterations in human tumors. Cancer Res 2001;61:7015–7019.

16 Boland CR, Thibodeau SN, Hamilton SR, Sidransky D, Eshleman JR, Burt RW, Meltzer SJ, Rodriguez-Bigas MA, Fodde R, Ranzani GN, Srivastava S: A National Cancer Institute workshop on microsatellite instability for cancer detection and familial predisposition: development of international criteria for the determination of microsatellite instability in colorectal cancer. Cancer Res 1998;58:5248–5257.

17 Lopes JM, Silva P, Seixas M, Cimes L, Seruca R: Microsatellite instability is not associated with degree of malignancy and p53 expression of gastrointestinal stromal tumours. Histopathology 1988;33:583–585.

18 Fukasawa T, Chong JM, Sakurai S, Koshiishi N, Ikeno R, Tanaka A, Matsumoto Y, Hayashi Y, Koike M, Fukuyama M: Allelic loss of 14q and 22q, *NF2* mutation, and genetic instability occur independently of c-*kit* mutation in gastrointestinal stromal tumor. Jpn J Cancer Res 2000;91:1241–1249.

19 Chinnery PF, Turnbull DM: Mitochondrial DNA and disease. Lancet 1999;354:s17–21.

20 Tan DJ, Bai RK, Wong LJ: Comprehensive scanning of somatic mitochondrial DNA mutations in breast cancer. Cancer Res 2002;62:972–976.

21 Hiyama T, Tanaka S, Shima H, Kose K, Kitadai Y, Ito M, Sumii M, Yoshihara M, Shimamoto F, Haruma K, Chayama K: Somatic mutation of mitochondrial DNA in *Helicobacter pylori*-associated chronic gastritis in patients with and without gastric cancer. Int J Mol Med 2003;12:169–174.

22 Larsson NG, Clayton DA: Molecular genetic aspects of human mitochondrial disorders. Annu Rev Genet 1995;29:151–178.

23 Habano W, Sugai T, Nakamaura S, Uesugi N, Yoshida T, Sasou S: Microsatellite instability and mutation of mitochondrial and nuclear DNA in gastric carcinoma. Gastroenterology 2000;118:835–841.

24 Hiyama T, Tanaka S, Shima H, Kose K, Tuncel H, Ito M, Kitadai Y, Sumii M, Yoshihara M, Shimamoto F, Haruma K, Chayama K: Somatic mutation in mitochondrial DNA and nuclear microsatellite instability in gastric cancer. Oncol Rep 2003;10:1837–1841.

25 Maximo V, Soares P, Seruca R, Rocha AS, Castro P, Sobrinho-Simoes M: Microsatellite instability, mitochondrial DNA large deletions, and mitochondrial DNA mutations in gastric carcinoma. Genes Chromosomes Cancer 2001;32:136–143.

26 Schwartz S, Perucho M: Somatic mutations in mitochondrial DNA do not associate with nuclear microsatellite instability in gastrointestinal cancer. Gastroenterology 2000;119:1806–1807.

27 Fang DC, Fang L, Wang RQ, Yang SM: Nuclear and mitochondrial DNA microsatellite instability in hepatocellular carcinoma in Chinese. World J Gastroenterol 2004;10:371–375.

Pathology International 2006; **56**: 200–205 doi:10.1111/j.1440-1827.2006.01946.x

Original Article

Molecular characteristics of differentiated-type gastric carcinoma with distinct mucin phenotype: LI-cadherin is associated with intestinal phenotype

Junichi Motoshita,[1,2] Hirofumi Nakayama,[1] Kiyomi Taniyama,[2] Keisuke Matsusaki[3] and Wataru Yasui[1]

[1]*Department of Molecular Pathology, Hiroshima University Graduate School of Biomedical Sciences,* [2]*Department of Clinical Laboratory, Pathology Division, National Hospital Organization, Kure Medical Center/Cnugoku Cancer Center, Kure and* [3]*Department of Surgery, Hofu Institute of Gastroenterology, Hofu, Japan*

Gastric carcinomas (GC) are classified into four phenotypes on the basis of the mucin expression profile: G type (gastric or foveolar phenotype), I type (intestinal phenotype), GI type (intestinal and gastric mixed phenotype) and N type (neither gastric nor intestinal phenotype). Immunohistochemistry was used to examine the expression of epidermal growth factor receptor (EGFR), E-cadherin, liver–intestine (LI)-cadherin, CD44v9 and p53 and correlation of these molecules with mucin phenotype and tumor stage was evaluated. Overexpression of EGFR and LI-cadherin, reduced expression of E-cadherin and abnormal expression of p53 were observed more frequently in advanced GC than in early GC. Among I-type GC, overexpression of EGFR and reduced expression of E-cadherin were observed more frequently in advanced tumors than in early tumors. Among G-type GC, reduced expression of E-cadherin was significantly associated with advanced tumors. With respect to the relationship between mucin phenotype and expression of cancer-related molecules, overexpression of LI-cadherin was observed more frequently in I-type (12/25, 48.0%) than in G-type (1/14, 7.1%) GC. I-type GC tended to express LI-cadherin more frequently than GI-type GC. These results provide insights into the molecular characteristics of the distinct mucin phenotype of differentiated-type GC and suggest that LI-cadherin may contribute to the biological behavior of I-type GC.

Key words: CD44v9, differentiated-type gastric carcinoma, E-cadherin, epidermal growth factor receptor, immunohistochemistry, liver–intestine-cadherin, mucin phenotype, p53, stomach

Gastric carcinomas (GC) are histologically classified into two major groups. Nakamura *et al.* described the 'differentiated' and 'undifferentiated' types[1] and Lauren described the 'intestinal' and 'diffuse' types based on glandular structure.[2] GC are also classified into four phenotypes on the basis of the mucin expression profile: G type (gastric or foveolar phenotype), I type (intestinal phenotype), GI type (intestinal and gastric mixed phenotype) and N type (neither gastric nor intestinal phenotype).[3–5] However, these classifications are confusing because of the presence of a gastric phenotype with the intestinal type of Lauren or the differentiated type, and of intestinal phenotypic cancers with diffuse structure.[5]

It has been suggested that G-type GC behave more aggressively than I-type GC.[6,7] Tatematsu *et al.* demonstrated, using a rat model, that the proportion of I-type cancer cells increased significantly as gastric lesions progressed from small to large differentiated-type GC.[5] Several distinct genetic differences have been reported between I-type and G-type GC. Mutations of p53 and loss of heterozygosity of the adenomatous polyposis coli (APC) gene occur more frequently in I-type GC than in G-type GC.[8–10] Microsatellite instability and alterations of the p73 gene were shown to be more common in G-type GC than in I-type GC.[11,12] Expression of mucin 2 (MUC2), a marker of intestinal epithelial cells, was associated with DNA methylation of human Mut L homolog 1 (hMLH1) and O^6-methylguanine-DNA methyltransferase (MGMT).[13] However, the molecular mechanism that underlies aggressive behavior of I-type GC remains unclear.

During the progression of GC, multiple genetic and epigenetic alterations accumulate.[14–16] These include overexpression of growth factors/receptors, abnormalities in cell cycle regulators and loss of cell adhesion molecules.[17] Abnormalities in the epidermal growth factor (EGF)/receptor system contribute to the malignant behavior of GC.[15] Loss of E-cadherin is associated with the invasive phenotype of GC.[15,18,19] The expression of CD44v9 is associated not only with tumor advancement but also with recurrence mortality of GC.[15,20] It was recently reported that overexpression of liver–intestine (LI)-cadherin, also known as cadherin-17, is associated with metastasis of GC to the lymph nodes.[21,22] We

Correspondence: Wataru Yasui, MD, PhD, Department of Molecular Pathology, Hiroshima University Graduate School of Biomedical Sciences, 1-2-3 Kasumi, Minami-ku, Hiroshima 734-8551, Japan. Email: wyasui@hiroshima-u.ac.jp

Received 16 August 2005. Accepted for publication 6 December 2005.

reported recently that expression of LI-cadherin correlates with tumor invasion and poor prognosis.[23]

To clarify the molecular characteristics of G-type and I-type differentiated-type GC, we examined the expression of cancer-related molecules such as epidermal growth factor receptor (EGFR), E-cadherin, LI-cadherin, CD44v9 and p53 and evaluated correlation with the mucin phenotypes and tumor stage.

MATERIALS AND METHODS

Tumor samples

Seventy-one samples of differentiated-type GC (38 early GC and 33 advanced GC) from 71 patients were studied. These samples were obtained by surgery at Hiroshima University Hospital or associated facilities between 1996 and 2000. The 71 tumors were classified as Ia ($n = 36$), Ib ($n = 11$), II ($n = 11$), IIIa ($n = 6$), IIIb ($n = 1$) and IV ($n = 6$) according to the post-surgical histopathological tumor, nodes, metastasis classification system (pTNM) classification system.[24] For immunohistochemical staining, tissues were fixed in 10% buffered-formalin and embedded in paraffin. Because written informed consent was not obtained, for strict privacy protection all identifying information was removed from samples prior to molecular expression analysis to protect patient privacy.

Phenotype analysis

GC were classified as G type, I type, GI type or N type according to the results of immunostaining for gastric-type markers (human gastric mucin (HGM) and mucin-recognizing gastric mucous cells (M-GGMC-1)) and intestinal-type markers (MUC2 and CD10) as described previously.[13] In brief, G type consisted of those samples in which >30% of the tumor cells were positive for gastric-type markers and showed little staining of intestinal-type markers. I type consisted of samples in which >30% of the tumor cells were positive for MUC2 or in which >5% of the tumor cells were positive for CD10 and showed little staining of gastric-type markers. GC showing positive staining for both gastric- and intestinal-type markers were classified as GI type, and those with no staining of any of the four markers were classified as N type. Among the 71 GC used in the present study, the mucin phenotype of the 33 advanced GC had been analyzed previously and reported elsewhere.[13]

Immunohistochemistry

Tissue sections (4 μm thick) were prepared from paraffin blocks, and representative sections were immunostained. Immunostaining was done by the immunoperoxidase techniques with a Histofine Simple Stain Kit (Nichirei Biosciences, Tokyo, Japan).[13] Deparaffinized tissue sections were immersed in methanol containing 3% hydrogen peroxide for 15 min to block endogenous peroxidase activity. Sections were microwaved in citrate buffer for 15–45 min to retrieve the antigenicity. Sections were then incubated with primary antibodies against the following antigens: HGM (1:50, NCL-HGM-45M1, Novocastra, Newcastle upon Tyne, UK), M-GGMC-1 (1:50, HIK1083, Kanto Kagaku, Tokyo, Japan), MUC2 (1:200, Ccp58, Santa Cruz Biotechnology, Santa Cruz, CA, USA), CD10 (1:50, NCL-CD10-270, Novocastra), E-cadherin (1:50, HECD-1, Takara Bio, Ohtsu, Japan), LI-cadherin (1:200, sc-6978, Santa Cruz Biotechnology) and p53 (1:100, NCL-p53-DO7, Novocastra), for 1.5 h at 37°C followed by incubation with the secondary antibody for 30 min. Immunocomplexes were then visualized with 3,3'-diaminobenzidine. Sections were counterstained with hematoxylin. For immunostaining of EGFR and CD44v9, a modified immunoglobulin enzyme bridge technique (avidin–biotin peroxidase complex method) was used as described previously.[25] Antibody against EGFR (1:50, NCL-EGFR.113, Novocastra) or antibody against CD44v9 (1:5000, NCL-CD44, Novocastra) was used.

Immunoreactivity was graded according to the number of cells stained and the intensity of the reaction in individual cells. Grades were assigned as follows: EGFR and CD44v9, tumors containing >5% immunoreactive tumor cells were considered positive (overexpression); LI-cadherin, tumors containing >25% immunoreactive tumor cells were considered positive (overexpression);[26] and E-cadherin, tumors containing <5% immunoreactive tumor cells were classified as having reduced expression.[27] For p53, staining was classified as: –, no staining; 1+, <20% of tumor cells stained either intensely or weakly; 2+, 20–50% of tumor cells stained intensely; and 3+, >50% of tumor cells stained intensely. Grades 1+, 2+ and 3+ were regarded as positive and indicated abnormal expression.

Statistics

Fisher's exact test was used for statistical analysis. $P < 0.05$ was regarded as statistically significant.

RESULTS

Mucin phenotypes of gastric carcinoma

The mucin phenotypes and tumor stages of the differentiated-type GC used in the present study and their tumor stage are summarized in Table 1. On the basis of the profile of

Table 1 Mucin phenotypes and tumor stage of differentiated-type GC used in the present study

Stage	G-type	I-type	GI-type	N-type	Total
Early	9	13	9	7	38
Advanced	5	14	9	5	33
TNM					
I, II	12	17	12	12	53
III, IV	2	10	6	0	18
Total	14	27	18	12	71

G-type, gastric or foveolar phenotype; GI-type, intestinal and gastric mixed phenotype; I-type, intestinal phenotype; N-type, neither gastric nor intestinal phenotype; TNM, tumor, nodes, metastases classification.

expression of the four mucin markers, we classified the 38 early GC as nine (23.7%) G-type, 13 (34.2%) I-type, nine (23.7%) GI-type, and seven (18.4%) N-type GC. The mucin phenotypes of the 33 advanced GC (5 (15.2%) G type, 14 (42.4%) I type, 9 (27.2%) GI type and 5 (15.2%) N-type) were reported previously.[13] Most G-type and all N-type GC were of stages I and II, whereas 10 of 27 (37.0%) I-type and six of 18 (33.3%) GI-type GC were of stages III and IV.

Correlation between expression of cancer-related molecules and tumor stage

We first compared the expression of cancer-related molecules between early and advanced differentiated-type GC. Representative staining patterns for EGFR, E-cadherin, LI-cadherin and p53 are shown in Fig. 1, and the overall results are summarized in Table 2. Overexpression of EGFR and LI-cadherin, reduced expression of E-cadherin and abnormal expression of p53 were observed more frequently among advanced GC than among early GC ($P = 0.000056$, $P = 0.00047$, $P = 0.015$ and $P = 0.013$, respectively). These results are consistent with those of previous reports.[15,23,28,29]

We then studied the relation between tumor stage and molecular expression for each mucin phenotype of differentiated-type GC. In general, aberrant expression of EGFR, E-cadherin, LI-cadherin and p53 tended to be more common in advanced tumors than in early tumors regardless of the mucin phenotype, except for LI-cadherin expression in GI-type and p53 expression in GI-type GC. There was no clear trend for CD44v9 expression. The following statistically significant correlations were detected: I-type GC, overexpression of EGFR and reduced expression of E-cadherin were observed more frequently in advanced tumors than in early tumors ($P = 0.0082$ and $P = 0.018$, respectively); G-type GC, reduced expression of E-cadherin was significantly associated with advanced cases ($P = 0.027$); and N-type GC advanced cases frequently showed overexpression of EGFR and LI-cadherin, whereas none of the early cases showed overexpression of these molecules. Because all N-type advanced GC were stage II cancers, no significant association between overexpression of EGFR and LI-cadherin and TNM stage was detected (data not shown).

Table 2 Expression of EGFR, E-cadherin, LI-cadherin, CD44v9 and p53 in differentiated-type GC

Phenotype	Early *n* (%)	Advanced *n* (%)	*P*†	Total *n* (%)
EGFR: overexpression				
G-type	0/8 (0)	2/5 (40.0)	0.13	2/13 (15.4)
I-type	2/13 (15.4)	9/13 (63.2)	0.0082	11/26 (42.3)
GI-type	1/8 (12.5)	3/9 (33.3)	0.58	4/17 (23.5)
N-type	0/7 (0)	3/5 (60.0)	0.045	3/12 (25.0)
Total	3/36 (8.3)	17/32 (53.1)	0.000056	20/68 (29.4)
E-cadherin: reduced expression				
G-type	0/9 (0)	3/5 (60.0)	0.027	3/14 (21.4)
I-type	2/13 (15.4)	11/14 (64.3)	0.018	11/27 (40.7)
GI-type	1/8 (12.5)	4/8 (50.0)	0.28	5/16 (31.2)
N-type	2/7 (28.6)	2/5 (40.0)	1.0	4/12 (33.3)
Total	5/37 (13.5)	18/32 (56.2)	0.00047	23/69 (33.3)
LI-cadherin: overexpression				
G-type	0/9 (0)	1/5 (20.0)	0.36	1/14 (7.1)
I-type	4/13 (30.8)	8/12 (66.7)	0.16	12/25 (48.0)
GI-type	2/8 (25.0)	1/8 (12.5)	1.0	3/16 (18.8)
N-type	0/7 (0)	4/5 (80.0)	0.01010	4/12 (33.3)
Total	6/37 (16.2)	14/30 (46.7)	0.015	20/67 (29.9)
CD44v9: overexpression				
G-type	5/9 (55.6)	3/5 (60.0)	1.0	8/14 (57.1)
I-type	5/13 (38.5)	9/13 (69.2)	0.24	14/26 (53.8)
GI-type	3/9 (33.3)	3/9 (33.3)	1.0	6/18 (33.3)
N-type	3/7 (42.9)	1/5 (20.0)	0.58	4/12 (33.3)
Total	16/38 (42.1)	16/32 (50.0)	0.51	32/70 (45.7)
p53: abnormal expression				
G-type	3/9 (33.3)	3/5 (60.0)	0.58	6/14 (42.9)
I-type	4/13 (30.8)	10/14 (71.4)	0.084	14/27 (51.9)
GI-type	5/9 (55.6)	4/9 (44.4)	1.0	9/18 (50.0)
N-type	1/7 (14.3)	4/5 (80.0)	0.072	5/12 (41.7)
Total	13/38 (34.2)	21/33 (63.6)	0.013	34/71 (47.9)

EGFR, epidermal growth factor receptor; GC, gastric carcinoma; G-type, gastric or foveolar phenotype; GI-type, intestinal and gastric mixed phenotype; I-type, intestinal phenotype; LI, liver–intestine; N-type, neither gastric nor intestinal phenotype.

Early, early GC; advanced, advanced GC.

†Fisher's exact test.

Association between mucin phenotype and expression of cancer-related molecules

Finally, we examined the relation between mucin phenotype and expression of cancer-related molecules. As shown in Table 3, there was a significant association between LI-cadherin expression and mucin phenotype. Overexpression of LI-cadherin was observed more frequently in I-type (12/25, 48.0%) than in G-type (1/14, 7.1%) GC ($P = 0.013$). Moreover, I-type GC tended to express LI-cadherin more frequently than GI-type GC ($P = 0.097$). No such trends were noticed for expression of EGFR, E-cadherin, CD44v9 and p53.

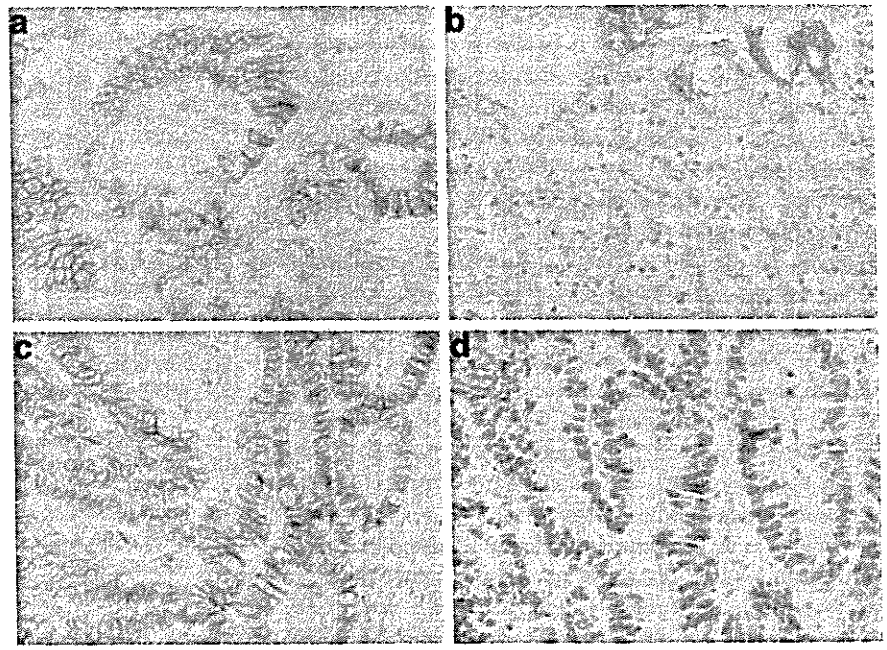

Figure 1 Representative immunohistochemical staining of epidermal growth factor receptor (EGFR), E-cadherin, liver–intestine (LI)-cadherin and p53 in differentiated-type gastric carcinomas (GC). (**a**) In the intestinal and gastric mixed phenotype (GI type) of advanced GC, EGFR is expressed in the cell membrane of many tumor cells. (**b**) In the gastric or foveolar phenotype (G type) of early GC, E-cadherin is expressed in the cell membrane of some tumor cells located superficially, and it is lost in many tumor cells. (**c**) In the intestinal phenotype (I-type) of advanced GC, LI-cadherin is uniformly expressed in cell membrane of most tumor cells. (**d**) In I-type early GC, almost all tumor cells express p53 in their nuclei.

Table 3 Correlation between mucin phenotype and expression of cancer-related molecules

Phenotype	*P*†				
EGFR	E-cadherin	LI-cadherin	CD44v9	p53	
G-type *vs* I-type	0.15	0.30	0.013	0.89	0.83
G-type *vs* GI-type	0.67	0.69	0.60	0.32	0.96
G-type *vs* N-type	0.64	0.67	0.15	0.41	0.74
I-type *vs* GI-type	0.35	0.77	0.097	0.30	0.86
I-type *vs* N-type	0.47	0.93	0.63	0.41	0.81
GI-type *vs* N-type	1.0	0.77	0.42	0.69	0.94

EGFR, epidermal growth factor receptor; GC, gastric carcinoma; G-type, gastric or foveolar phenotype; GI-type, intestinal and gastric mixed phenotype; I-type, intestinal phenotype; LI, liver–intestine; N-type, neither gastric nor intestinal phenotype.
†Fisher's exact test.

DISCUSSION

To clarify the molecular bases of possible biological differences between the mucin phenotypes of GC, we examined expression of representative molecules associated with invasion and metastasis. Our present data for the relation between molecular expression and tumor stage in all of our differentiated-type GC were consistent with the results of previous studies.[15,23,28,29] With respect to specific mucin phenotypes, the expression profiles of certain molecules had statistically significant associations with tumor stage. Among I-type GC, overexpression of EGFR and reduced expression of E-cadherin were detected more frequently in advanced tumors than in early tumors. Among G-type GC, reduced expression of E-cadherin was significantly associated with advanced tumors. Therefore, loss of E-cadherin may be associated with invasion and progression of both G-type and I-type GC, whereas overexpression of EGFR may participate strongly in I-type GC.

Examination of the relationship between expression of specific molecules and mucin phenotypes revealed a significant difference in the expression of LI-cadherin between phenotypes. Overexpression of LI-cadherin was observed more frequently in I-type than in G-type GC, and there was a tendency for I-type GC to express LI-cadherin more frequently than GI-type GC. These results suggest that LI-cadherin may contribute to distinct biological behaviors of I-type GC. LI-cadherin is a structurally unique member of the cadherin superfamily.[30,31] LI-cadherin has only 20 amino acids in the cytoplasmic domain, whereas classical cadherins have a highly conserved cytoplasmic domain that consists of 150–160 amino acids. We previously examined gene expression profiles of GC by serial analysis of gene expression and found that LI-cadherin was one of the most

upregulated genes in the advanced GC, and the levels of expression as measured by quantitative reverse transcription–polymerase chain reaction were significantly associated with tumor invasion.[32–34] Although it has been reported that LI-cadherin is expressed in some intestinal metaplasias and the intestinal-type GC of Lauren,[21–23] to our knowledge this is the first demonstration that LI-cadherin expression is significantly associated with I-type GC.

Caudal-type homeobox (CDX) 1 and CDX2 are members of the caudal-related homeobox gene family, and CDX proteins act as intestine-specific transcription factors and increase expression of goblet-specific MUC2 gene.[34,35] Expression of CDX1 and CDX2 is strongly associated with intestinal metaplasia and I-type GC.[5,34,36] CDX2 binds to the promoter of the LI-cadherin gene and upregulates gene expression.[37] However, unlike classical cadherins, in which reduced expression is associated with tumor progression, the mechanism by which overexpression of LI-cadherin is associated with tumor progression remains unknown. Biological study should be performed in the near future.

In conclusion, our results provide some molecular characterization of the distinct mucin phenotypes of differentiated-type GC and suggest that LI-cadherin may be associated with the biological behavior of I-type GC.

ACKNOWLEDGMENTS

This work was supported, in part, by Grants-in-Aid from the Ministry of Education, Culture, Sports, and Technology of Japan, and the Ministry of Health, Labor, and Welfare of Japan. The authors thank Masayoshi Takatani, Hiroshima University, and staff members of the Division of Pathology and Cytology, Hiroshima City Medical Association Clinical Laboratories, for their skillful technical assistance.

REFERENCES

1 Nakamura K, Sugano H, Takagi K. Carcinoma of the stomach in incipient phase: Its histogenesis and histological appearance. *Gann* 1968; **59**: 251–8.
2 Lauren P. The two histological main types of gastric carcinoma: Diffuse and so-called intestinal type carcinoma: An attempt at histological classification. *Acta Pathol Microbiol Scand* 1965; **64**: 31–49.
3 Fiocca R, Villani L, Tenti P *et al.* Characterization of four main cell types in gastric cancer: Foveolar, mucopeptic, intestinal columnar and goblet cells: An histopathologic, histochemical and ultrastructual study of 'early' and 'advanced' tumours. *Pathol Res Pract* 1987; **182**: 308–25.
4 Tatematsu M, Tsukamoto T, Inada K. Stem cells and gastric cancer: Role of gastric and intestinal mixed intestinal metaplasia. *Cancer Sci* 2003; **94**: 135–41.
5 Tatematsu M, Tsukamoto T, Mizoshita T. History of gastric carcinoma research in Japan: Basic aspects. In: Kaminishi M, Takubo K, Mafune K, eds. *The Diversity of Gastric Carcinoma Pathogenesis: Diagnosis, and Therapy*. Tokyo: Springer, 2005; 3–28.
6 Koseki K, Takizawa T, Koike M, Ito M, Nihei Z, Sugihara K. Distinction of differentiated type early gastric carcinoma with gastric type mucin expression. *Cancer* 2000; **89**: 724–32.
7 TajimaY, Shimoda T, Nakanishi Y *et al.* Gastric and intestinal phenotypic marker expression in gastric carcinomas and its prognostic significance: Immunohistochemical analysis of 136 lesions. *Oncology* 2001; **61**: 212–20.
8 Endoh Y, Sakata K, Tamura G *et al.* Cellular phenotypes of differentiated-type adenocarcinomas and precancerous lesions of the stomach are dependent on the genetic pathways. *J Pathol* 2000; **191**: 257–63.
9 Kushima R, Muller W, Stolte M, Borchad F. Differential p53 protein expression in stomach adenomas of gastric and intestinal phenotypes: Possible sequences of p53 alteration in stomach carcinogenesis. *Virchows Arch* 1996; **428**: 223–7.
10 Wu LB, Kushima R, Borchard F, Molsberger G, Hattori T. Intramucosal carcinomas of the stomach: Phenotypic expression and loss of heterozygosity at microsatellites linked to the APC gene. *Pathol Res Pract* 1998; **194**: 405–11.
11 Shibata N, Watari J, Fujiya M, Tanno S, Saitoh Y, Kohgo Y. Cell kinetics and genetic instabilities in differentiated type early gastric cancers with different mucin phenotype. *Hum Pathol* 2003; **34**: 32–40.
12 Yokozaki H, Shitara Y, Fujimoto J, Hiyama T, Yasui W, Tahara E. Alterations of p73 preferentially occur in gastric adenocarcinomas with foveolar epithelial phenotype. *Int J Cancer* 1999; **83**: 192–6.
13 Motoshita J, Oue N, Nakayama H *et al.* DNA methylation profiles of differentiated-type gastric carcinomas with distinct mucin phenotypes. *Cancer Sci* 2005; **96**: 474–9.
14 Yasui W, Oue N, Kitadai Y *et al.* Recent advances in molecular pathobiology of gastric carcinoma. In: Kaminishi M, Takubo K, Mafune K, eds. *The Diversity of Gastric Carcinoma Pathogenesis: Diagnosis, and Therapy*. Tokyo: Springer, 2005; 51–71.
15 Yokozaki H, Yasui W, Tahara E. Genetic and epigenetic changes in stomach cancer. *Int Rev Cytol* 2001; **204**: 49–95.
16 Yasui W, Oue N, Ono S, Mitani Y, Ito R, Nakayama H. Histone acetylation and gastrointestinal carcinogenesis. *Ann NY Acad Sci* 2003; **983**: 220–31.
17 Yasui W, Oue N, Aung PP, Matsumura S, Shutoh M, Nakayama H. Molecular-pathobiological prognostic factors of gastric cancer: A review. *Gastric Cancer* 2005; **8**: 86–94.
18 Shimada Y, Yamasaki S, Hashimoto Y *et al.* Clinical significance of dysadherin expression in gastric cancer patients. *Clin Cancer Res* 2004; **10**: 2818–23 (Erratum: *Clin Cancer Res* 2004; **10**: 4198).
19 Chen HC, Chu RY, Hsu PN *et al.* Loss of E-cadherin expression correlates with poor differentiation and invasion into adjacent organs in gastric adenocarcinomas. *Cancer Lett* 2003; **201**: 97–106.
20 Mayer B, Jauch KW, Gunthert U *et al.* De-novo expression of CD44 and survival in gastric cancer. *Lancet* 1993; **342**: 1019–22.
21 Ko S, Chu KM, Luk JM *et al.* Overexpression of LI-cadherin in gastric cancer is associated with lymph node metastasis. *Biochem Biophys Res Commun* 2004; **319**: 562–8.
22 Ko S, Chu KM, Luk JM *et al.* CDX2 co-localized with liver-intestine cadherin in intestinal metaplasia and adenocarcinoma of the stomach. *J Pathol* 2005; **205**: 615–22.
23 Ito R, Oue N, Yoshida K *et al.* Clinicopathological significant and prognostic influence of cadherin-17 expression in gastric cancer. *Virchows Arch* 2005; **447**: 717–22.

24 Sobin LH, Wittekind CH, eds. *TNM Classification of Malignant Tumors*, 6th edn. New York: Wiley-Liss, 2002.
25 Yasui W, Akama Y, Kuniyasu H *et al.* Expression of cyclin-dependent kinase inhibitor p21WAF1/CIP1 in non-neoplastic mucosa and neoplasia of the stomach: Relation with p53 status and proliferative activity. *J Pathol* 1996; **180**: 122–8.
26 Takamura M, Sakamoto M, Ino Y *et al.* Expression of liver-intestine cadherin and its possible interaction with galectin-3 in ductal adenocarcinoma of the pancreas. *Cancer Sci* 2003; **94**: 425–30.
27 Shimoyama Y, Hirohashi S. Expression of E- and P-cadherin in gastric carcinoma. *Cancer Res* 1991; **51**: 2185–92.
28 Yasui W, Hata J, Yokozaki H *et al.* Interaction between epidermal growth factor and its receptor in progression of human gastric carcinoma. *Int J Cancer* 1988; **41**: 211–17.
29 Ito R, Nakayama H, Yoshida K, Matsumura S, Oda N, Yasui W. Expression of Cbl linking with the epidermal growth factor receptor system is associated with tumor progression and poor prognosis of human gastric carcinoma. *Virchows Arch* 2004; **444**: 324–31.
30 Berndorff D, Gessner R, Kreft B *et al.* Liver-intestine cadherin: Molecular cloning and characterization of a novel Ca^{2+}-dependent cell adhesion molecule expressed in liver and intestine. *J Cell Biol* 1994; **125**: 1353–69.
31 Dantzig A, Hoskins J, Tabas L *et al.* Association of intestinal peptide transport with a protein related to the cadherin superfamily. *Science* 1994; **264**: 430–33.
32 Oue N, Hamai Y, Mitani Y *et al.* Gene expression profile of gastric carcinoma: Identification of genes and tags potentially involved in invasion, metastasis, and carcinogenesis by serial analysis of gene expression. *Cancer Res* 2004; **64**: 2397–405.
33 Yasui W, Oue N, Ito R, Kuraoka K, Nakayama H. Search for new biomarkers of gastric cancer through serial analysis of gene expression and its clinical implications. *Cancer Sci* 2004; **95**: 385–92.
34 Almeida R, Silva E, Santos-Silva F *et al.* Expression of intestine-specific transcription factors, CDX1 and CDX2, in intestinal metaplasia and gastric carcinomas. *J Pathol* 2003; **199**: 36–40.
35 Yamamoto H, Bai YQ, Yuasa Y. Homeodomain protein CDX2 regulates goblet-specific MUC2 gene expression. *Biochem Biophys Res Commun* 2003; **300**: 813–18.
36 Eda A, Osawa H, Yanaka I *et al.* Expression of homeobox gene CDX2 precedes that of CDX1 during the progression of intestinal metaplasia. *J Gastroenterol* 2002; **37**: 94–100.
37 Hinoi T, Lucas PC, Kuick R, Hanash S, Cho KR, Fearon ER. CDX2 regulates liver intestine-cadherin expression in normal and malignant colon epithelium and intestinal metaplasia. *Gastroenterology* 2002; **123**: 1565–7.

tumour was not of endometrioid subtype. Papers were excluded if they consisted of cases that had been included in other studies, had no follow-up or were in a foreign language with no English translation. A case of carcinomatous transformation in a focus of adenomyosis was excluded. It is perhaps a little disappointing that none of the series included control groups with which the outcome of these patients could have been compared, but this may reflect the difficulty of defining such groups in pathology series.

A total of 136 cases were recorded. Following aggregation of the data, 41 cases had residual or recurrent atypical polypoid adenomyoma [30.1%, confidence interval (CI) 23.1, 38.8], 12 had evidence of background endometrial hyperplasia (8.8%) and 12 had endometrial adenocarcinoma (8.8%, CI 23.1, 38.8). Carcinoma was identified in the adjacent endometrium in three cases, whilst in the remaining nine cases the carcinoma was located within the atypical polypoid adenomyoma or in association with its base.

Aggregating the published series indicates an average risk of endometrial carcinoma in women with atypical polypoid adenomyoma of 8.8%, which is considerably higher than the overall risk of 0.8% reported in a recent series of endometrial polyps,[2] although this increased to 32.6% (24.3–41.2%) in another series[3] of women with polyps aged over 65 years but is less than that described in complex atypical hyperplasia, where an overall frequency of cancer of up to 45% has been described.[4,5] Persistence of complex atypical hyperplasia has been described in 14% of cases,[5] whilst in atypical polypoid adenomyoma it was 8.8%.

These results have originated from a variety of case reports and series described over the years by pathologists, many with recognized expertise in gynaecological pathology and indicate that in some cases at least, atypical polypoid adenomyoma is associated with adenocarcinoma, suggesting that this lesion should be carefully evaluated and cannot be automatically regarded as being a totally benign entity. The presence of recurrent or residual atypical polypoid adenomyoma in 30.1% of the cases described would seem to indicate a continued risk for the development of malignant disease in patients in whom complete excision of the atypical polypoid adenomyoma cannot be guaranteed.

M K Heatley

Department of Histopathology, St James' University Hospital, Leeds, UK

1. Mazur MT. Atypical polypoid adenomyomas of the endometrium. *Am. J. Surg. Pathol.* 1981; 5; 473–482.
2. Savelli L, De Iaco P, Santini D *et al.* Histopathologic features and risk factors for benignity, hyperplasia, and cancer in endometrial polyps. *Am. J. Obstet. Gynecol.* 2003; 188; 927–931.
3. Hileeto D, Fadore O, Martel M, Zheng W. Endometrial polyp associated with increased risk of cancer involvment in postmenopausal women. *Mod. Pathol.* 2004; 17 (Suppl. 1); 198A.
4. Baak JPA, Wisse-Brekelmans ECM, Fleege JC, van der Putten HWHM, Bezemer JC. Assessment of the risk on endometrial cancer in hyperplasia, by means of orphological and morphometrical features. *Pathol. Res. Pract.* 1992; 188; 856–859.
5. Kurman RJ, Kaminski PF, Norris HJ. The behaviour of endometrial hyperplasia. *Cancer* 1985; 56; 403–412.

Lack of pericryptal fibroblastic cells adjacent to intestinal epithelial metaplastic gastric glands

DOI: 10.1111/j.1365-2559.2005.02271.x

Sir: In colorectal mucosa, fibroblasts are located in two different sites, randomly distributed throughout the lamina propria or in the pericryptal fibroblast sheath surrounding the crypts and in the most superficial portion of the lamina propria, tightly apposed to the subepithelial basement membrane complex.[1,2] Fibroblasts in the pericryptal areas, namely pericryptal fibroblasts (PCFs), express not only α-smooth muscle actin (ASMA) but also, high-molecular-weight caldesmon (HCD), suggesting that PCFs are well-differentiated pericryptal smooth muscle cells rather than pericryptal myofibroblasts/fibroblasts.[3] Colorectal PCFs play an important role in the inhibition of tumorigenesis and tumour invasion[4–6] and progression of inflammatory bowel disease to dysplasia.[7]

In order to examine the distribution of PCFs in areas adjacent to intestinal epithelial metaplasia in gastric mucosa, we performed immunostaining for HCD in gastric mucosa with intestinal epithelial metaplasia. A total of 51 gastric neoplastic tissues and associated non-neoplastic mucosa (28 surgically resected intestinal-type gastric carcinomas and 23 endoscopically resected gastric adenomas and their non-neoplastic tissues) from the Surgical Pathology Files of the Department of Pathology, Kochi Medical School, Kochi University and its affiliated hospitals from 1994 to 2002 were examined. All of the 51 non-neoplastic gastric tissues contained areas of intestinal epithelial metaplasia. The definitions used for histological classification were based on the criteria of Lauren[8] and our previous report.[9] Immunohistochemical studies were performed using a Histofine SAB-PO (multi) kit

(Nichirei, Tokyo, Japan). A monoclonal antibody against HCD (clone h-CD; Dakopatts (Glostrup, Denmark), 1 : 50 dilution, microwave treatment) was used.[3] We regarded HCD-positive stromal cells adjacent to glands to be PCFs.[3] Vascular media and muscularis mucosa served as positive controls for HCD.

No HCD-positive stromal cells were detected adjacent to intestinal epithelial metaplastic gastric glands in any of the cases examined, i.e. no PCFs were detected adjacent to intestinal epithelial metaplastic gastric glands (Figure 1). HCD-positive thin smooth muscle bundles arising from the muscularis mucosa and extending vertically up to the surface of the mucosa were detected (Figure 1). No HCD-positive stromal cells were observed in the areas adjacent to non-neoplastic non-metaplastic gastric glands (not shown). As in the gastric mucosa with intestinal metaplasia, HCD-positive thin smooth muscle bundles arising from the muscularis mucosa and extending vertically up to the surface of the mucosa were seen (not shown). No HCD-positive stromal cells were detected in the areas adjacent to neoplastic glands (not shown).

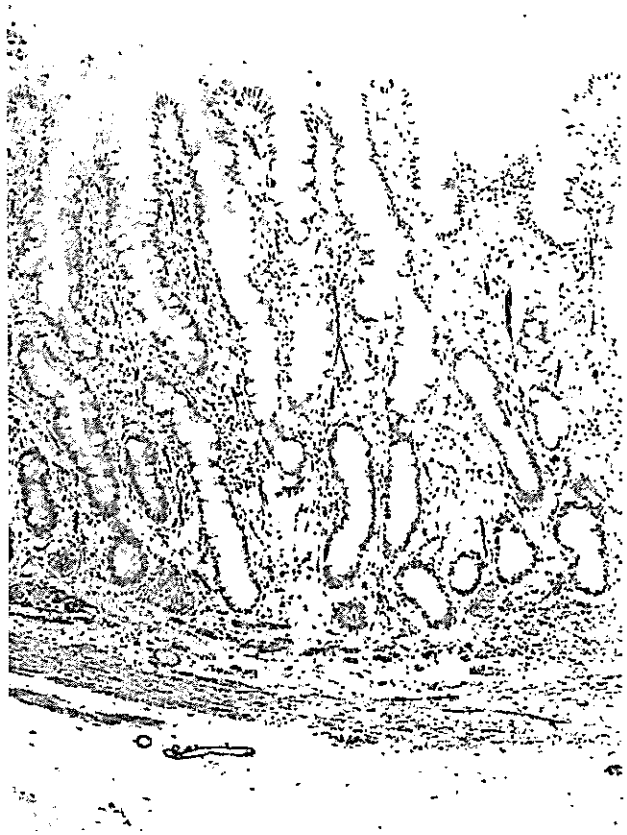

Figure 1. Immunoreactivity for high-molecular-weight caldesmon (HCD) in gastric mucosa with intestinal metaplasia. No HCD-positive stromal cells are detected in the areas adjacent to intestinal epithelial metaplastic gastric glands: HCD is positive in thin smooth muscle bundles extending from the muscularis mucosa vertically up to the surface of the mucosa.

Fetal gut mesenchymal cells modulate epithelial cell differentiation.[4] Reciprocal stromal–epithelial interactions in the digestive tract are maintained beyond embryonic life;[4] mature colonic mucosa contains PCFs exhibiting smooth muscle morphological features and regulating the growth and differentiation of adjacent epithelial cells.[4]

Reduction of PCFs is associated with colorectal tumorigenesis and tumour progression. PCFs gradually decrease in the sequence of adenoma, intramucosal carcinoma, and submucosal invasive carcinoma.[5] Depressed adenomas are considered to be a subtype of flat adenomas.[6] The depletion of PCFs seems to correlate with the depressed growth of colorectal adenoma.[6] Reduction of PCFs in background mucosa may relate to the development of villous change and dysplasia in ulcerative colitis.[7]

Intestinal metaplasia is proposed to be a precancerous lesion of intestinal-type gastric carcinoma.[8] In the present study, no PCFs surrounding intestinal epithelial metaplastic gastric glands were detected. Neoplastic intestinal-type gastric glands also have no accompanying PCFs. The stromal environment adjacent to intestinal epithelial metaplastic gastric glands may be similar to that adjacent to colorectal depressed adenoma glands, but quite different from that adjacent to normal colorectal crypts. There is a possibility that the stromal environment lacking PCFs makes intestinal epithelial metaplastic gastric glands unstable. Thin bundles of smooth muscle from the muscularis mucosa penetrate into the lamina propria.[3] These smooth muscle cells are not PCFs.[10]

In conclusion, intestinal metaplasia is intestinal epithelial metaplasia without PCFs. There is a possibility that lack of PCFs is associated with gastric epithelial tumorigenesis. Further molecular and biological investigations are needed into those areas adjacent to intestinal epithelial metaplastic gastric glands.

H Nakayama
H Enzan[1]
W Yasui

Department of Molecular Pathology, Graduate School of Biomedical Sciences, Hiroshima University, Hiroshima, and
[1]*Department of Pathology, Kochi Medical School, Kochi University, Kochi, Japan*

 Histopathology, 48, 605–626.

1. Levine DS, Haggitt RC. Colon. In Sternberg SS ed. *Histology for pathologists*, 2nd edn. Philadelphia: Lippincott-Raven Publishers 1997; 519–537.
2. Kaye GI, Pascal RR, Lane N. The colonic pericryptal fibroblast sheath: replication, migration, and cytodifferentiation of a mesenchymal cell system in adult tissue. III. Replication and differentiation in human hyperplastic and adenomatous polyps. *Gastroenterology* 1971; 60; 515–536.
3. Nakayama H, Miyazaki E, Enzan H. Differential expression of high-molecular-weight caldesmon in colorectal pericryptal fibroblasts and tumor stroma. *J. Clin. Pathol.* 1999; 52; 785–786.
4. Sappino AP, Dietrich PY, Skalli O, Widgren S, Gabbiani G. Colonic pericryptal fibroblasts. Differentiation pattern in embryogenesis and phenotypic modulation in epithelial proliferative lesions. *Virchows Arch. A Pathol. Anat. Histopathol.* 1989; 415; 551–557.
5. Yao T, Tsuneyoshi M. Significance of pericryptal fibroblasts in colorectal epithelial tumors: a special reference to the histologic features and growth patterns. *Hum. Pathol.* 1993; 24; 525–533.
6. Yao T, Tada S, Tsuneyoshi M. Colorectal counterpart of gastric depressed adenoma. A comparison with flat and polypoid adenomas with special reference to the development of pericryptal fibroblasts. *Am. J. Surg. Pathol.* 1994; 18; 559–568.
7. Yao T, Talbot IC. The demonstration of pericryptal fibroblasts in background mucosa and dysplasia complicating ulcerative colitis. *Histopathology* 1996; 28; 325–331.
8. Lauren P. The two main types of gastric carcinoma. Diffuse and so-called intestinal type carcinomas. *Acta Pathol. Microbiol. Scand.* 1965; 64; 31–49.
9. Nakayama H, Enzan H, Miyazaki E, Toi M. Alpha smooth muscle actin positive stromal cells in gastric carcinoma. *J. Clin. Pathol.* 2002; 55; 741–744.
10. Mutoh H, Sakurai S, Satoh K *et al.* Pericryptal fibroblast sheath in intestinal metaplasia and gastric carcinoma. *Gut* 2005; 54; 33–39.

Expression of CD73 and its ecto-5′-nucleotidase activity are elevated in papillary thyroid carcinomas

DOI: 10.1111/j.1365-2559.2005.02277.x

Sir: CD73, known as ecto-5′-nucleotidase, is a glycosylphosphatidylinositol-linked 70-kDa molecule whose enzymatic activity involves catalysing the dephosphorylation of ribo- and deoxyribonucleotide 5′-monophosphates to their corresponding nucleosides. This surface antigen may regulate the availability of adenosine for interaction with the cell surface adenosine

Figure 1. Immunohistochemistry for CD73. A, Papillary thyroid carcinoma. CD73 is strongly immunopositive at the apical cell membrane. B, Normal thyroid. CD73 is negative in follicular epithelial cells, while endothelial cells are immunopositive. C, Nodular goitre. CD73 is immunonegative in hyperplastic follicular epithelial cells which are forming papillary structures. D, Follicular adenoma. CD73 is immunonegative in benign neoplastic follicular epithelial cells which are forming follicle structures.

